DESIGN AND CONTROL OF THE DIELECTRIC PROPERTIES OF METAL-POLYMER BASED ARTIFICIAL NANODIELECTRICS FOR EMBEDDED CAPACITOR APPLICATIONS

A Thesis

Presented to

the Faculty of the Department of Electrical and Computer Engineering

University of Houston

In Partial Fulfillment

of the Requirements for the Degree of

Master of Science

in Electrical Engineering

by

Narasimha Reddy Ettedi

December 2013

DESIGN AND CONTROL OF THE DIELECTRIC PROPERTIES OF METAL-POLYMER BASED ARTIFICIAL NANODIELECTRICS FOR EMBEDDED CAPACITOR APPLICATIONS

Narasimha Reddy Ettedi

Approved:

Chairman of the Committee
Dr. Jiming Bao,
Assistant Professor
Electrical and Computer Engineering

Committee Members:

Research Advisor
Dr. Abdelhak Bensaoula,
Research Professor
Electrical and Computer Engineering

Dr. David Starikov,
Research Associate Professor
Physics

Dr. Suresh Khator,
Associate Dean
Cullen College of Engineering

Dr. Badri Roysam,
Professor and Chairman
Electrical and Computer Engineering

ACKNOWLEDGEMENTS

Foremost, I would like to express my sincere gratitude to my advisor Dr. Abdelhak Bensaoula for the continuous support of my Masters research, for his patience, motivation, enthusiasm, and immense knowledge. His guidance helped me during the time of my research and the writing of this thesis. I could not have imagined having a better advisor and mentor for my Masters Thesis.

Besides my advisor, I would like to thank the rest of my thesis committee: Dr. Jiming Bao, and Dr. David Starikov, for their encouragement, insightful comments, and hard questions.

I thank my fellow lab mates in Nitride Devices and Materials Group at University of Houston for their continuous moral support and encouragement. A special thanks to Rajeev Pillai and Jateen Gandhi for their constant source of inspiration, training with the instruments, persistent help with measurements and stimulating me to learn the core concepts of device fabrication and characterization.

Last but not the least, I would like to thank my family: my parents and siblings for supporting me morally and spiritually throughout my life.

DESIGN AND CONTROL OF THE DIELECTRIC PROPERTIES OF METAL-POLYMER BASED ARTIFICIAL NANODIELECTRICS FOR EMBEDDED CAPACITOR APPLICATIONS

An Abstract

of a

Thesis

Presented to

the Faculty of the Department of Electrical and Computer Engineering

University of Houston

In Partial Fulfillment

of the Requirements for the Degree of

Master of Science

in Electrical Engineering

by

Narasimha Reddy Ettedi

December 2013

ABSTRACT

Extensive research is being done today on embedded capacitors because of their promising applications in energy storage solutions, microelectronics products, and packaging. However, selection of materials and process issues have been the stumbling blocks for commercialization of the embedded capacitor technology for electronic packages.

Polymer composite materials based on conductive nanoparticles provide a potential solution to embedded capacitors with the advantage of the polymers being compatible with standard printed circuit boards (PCB). Polymer nanocomposites with embedded nanoparticles have recently been investigated as potential materials with the capability of obtaining very high dielectric constant materials. This thesis work involves loading of Ag nanoparticles in a Polyvinylpyrrolidone (PVP) matrix and controlling the dielectric performance of this material system by employing methods such as controlled dispersion, centrifugation of agglomerated nanoparticles, multi-layered dielectric films and overall optimization of the material coating process. The dielectric behaviors of the nanocomposites were studied systematically over a range of frequencies to determine the dependence of dielectric constant, dielectric loss tangent and dielectric strength on these parameters. Percolation theory was used to analytically calculate K value of the composites. Finite Element Method (FEM)-based COMSOL Multiphysics simulations demonstrated an increase in the K value of composite.

TABLE OF CONTENTS

LIST OF FIGURES

LIST OF TABLES

CHAPTER 1. INTRODUCTION

1.1 Electronic systems

All electronic packaging systems consist of active and passive components on an interconnecting substrate [1]. Passive components are a class of electronic components that result in no power gain to an electronic application. Passive components typically provide charge storage, current-voltage phase angle, and impedance in an electronic circuit. Resistors, inductors and capacitors are some examples of passive components. Active components are those which rely on a source of energy, and contribute to power gain in an electronic circuit. Vacuum tubes, power sources and semiconductor devices like diodes and transistors are some examples of active devices.

In electronic circuit boards currently employed such as in cell phones, the ratio of passive components to active components is nearly 20:1, and about 80% of the circuit board area is occupied by discrete passive components [1]. Surface mounted discrete passive devices typically account for 30% of the solder joints and take up to 90% of the placement time during electronic assembly [2]. As a result, discrete passive devices contribute to large circuit board size, high cost and processing times and also reduced electrical performance. These effects are more dominant in modern electronic systems which use large number of discrete passive components to accomplish sophisticated tasks. Efforts are currently made by researchers to reduce the number of discrete passive devices on the surface of the substrate boards by embedding them into the inner layers of the circuit board.

1.2 Electronic packaging technologies

An electronic package is the portion of an electronic structure that protects an electronic/electrical element and its environment from each other [3]. Packaging is the bridge that interconnects the ICs and other components into a system-level board to form electronic products. The functions of an electronic package are to protect, power, and cool the microelectronic device and to provide an electrical and mechanical connection between the chip and the outside world. In addition to these requirements, an electronic package must be consistent with requirements for a high quality, reliable, serviceable, and economical product at its designed performance level.

As electronic products continue to miniaturize, increase in performance, and broaden in applications, it will be necessary to improve electronic packaging technologies to enable tomorrow's electronic systems. Consequently, electronic packaging has become the focus of an intense development effort and the challenge of the microelectronics industry today [4]. The figure below shows the evolution of electronic packaging over the years [7].

In the early 1950s, the single-chip packages were hermetically sealed metal cans with 2-10 legs or pins, which were mounted into holes on a printed wiring board (PWB). With the introduction of IC's in the early 1960s, it created a need for higher pin-count packages. The dual in-line package (DIP) was developed which provided more pins than a metal can, while allowing through-hole assembly in conventional circuit boards. In 1980s, DIPs began to be replaced by surface mount packages (SMPs) like Quad Flat Packages (QFPs) to provide higher density PWBs. The early 1990s saw the emergence of pin-grid array (PGA) and ball-grid array (BGA), because of their high I/O density,

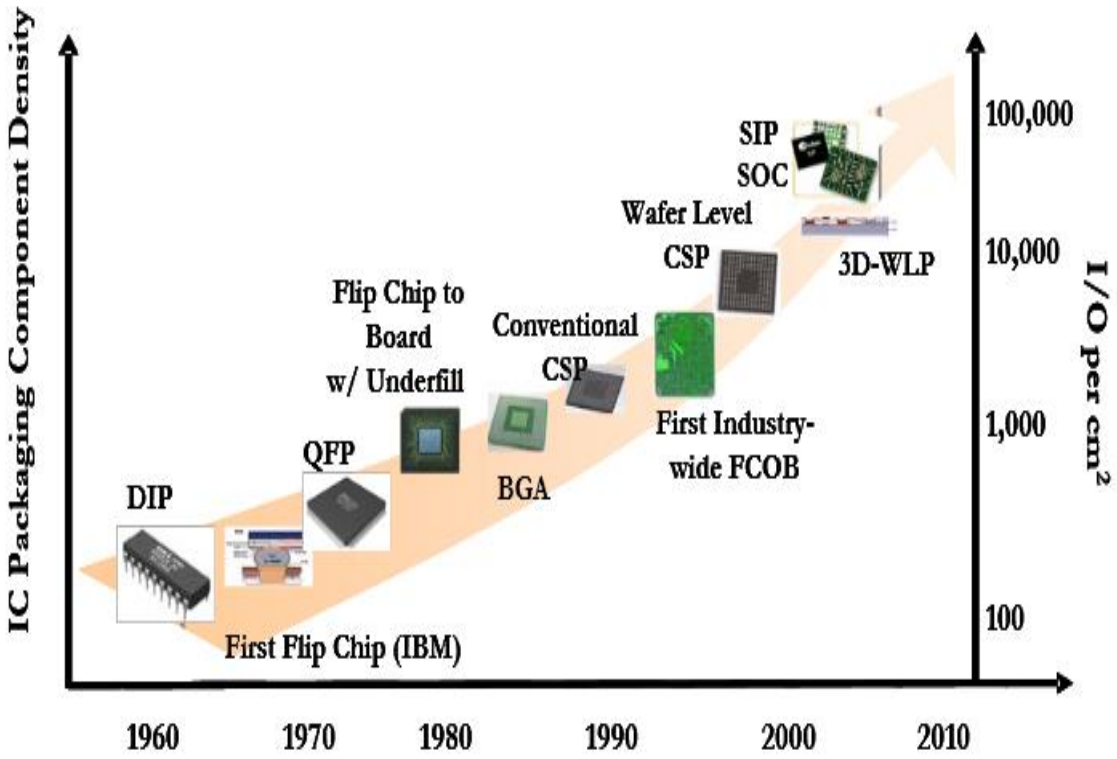

Figure 1.1 Evolution of electronic packaging.

minimized footprint, and better electrical performance. The most advanced technology in packaging called wafer level packaging (WLP) was introduced in late 1990s, and had power and signal redistributions and packaging protections onto the wafer. The future of packaging lies in system-level integrated package and 3-dimensional (3D) packaging.

1.3 Embedded passives

The electronic packaging industry is driven by the demand for miniaturization, better performance at low cost and increased functionality. Embedded passives can address the issues associated with surface mounted discrete passives. Embedded passive technology is realized by building passive components directly into the layers of laminate substrate. Figure 1.2 below shows an illustration of the embedded resistors and capacitors.

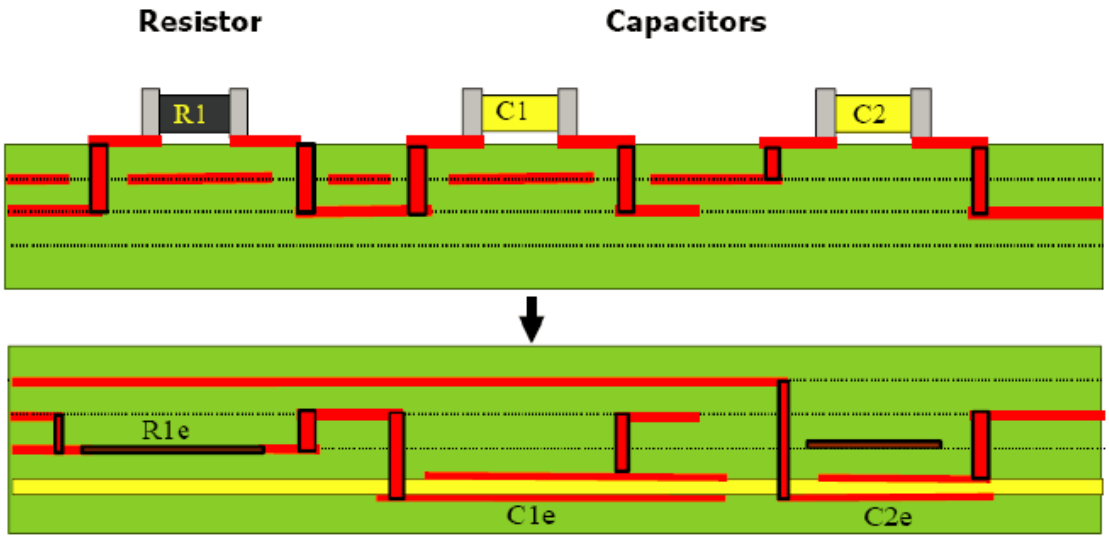

Figure 1.2 Schematic of embedded passives integrated into substrate.

Embedded passives provide numerous advantages compared to discrete passives. By embedding them into the inner layers of the substrate board, embedded passives not only reduce the size and weight of the passives and the overall board, but also provide benefits such as increased reliability, improved electrical performance and reduced cost. Embedded passives have considerably less parasitic effects compared to their discrete counterparts due to the lack of leads and contacts. Employing embedded passives in circuits also provides reliability advantage because two solder joints per device are eliminated, which are major points of failure for systems with discrete components [5].

1.4 Embedded capacitors

Capacitors are the most important of passive devices because of their devoted use in applications such as noise suppression, filtering, tuning, decoupling, bypassing, termination, and frequency determination. The number of passive devices per package is increasing steadily, with capacitors dominating in numbers among different types of passive components and their wide applications. Discrete capacitors occupy substantial

geometric surface area on the board, induce parasitic inductance, resistance and reduce electrical performance. Embedded capacitors provide solutions to some of these issues, since they may be shielded by ground electrodes and voltage supply electrodes, are leadless, and do not have solder joints. However, embedded capacitor technology has not yet been commercialized fully for electronic packages due to materials and process issues [51]. Therefore, it is necessary to develop materials that satisfy the requirements of fabrication as well as electrical and mechanical performances to enable embedded capacitor technology [6]. There is a huge research on the dielectric material, film formation methods and capacitor topography for embedded capacitor applications.

1.5 Challenges in selecting materials for embedded capacitors

A material ideal for embedded capacitors must possess a high dielectric constant with a low dissipation factor and must be compatible with printed circuit boards (PCBs). Such a material however, has not been developed. Polymer materials are arguably the most promising choice for embedded capacitor materials, but they have low dielectric constants. This problem can be overcome by adding fillers to the polymer that increase the effective dielectric constant of the composite. Ideally, the filler would enhance only the dielectric constant (K) but not the dielectric loss. Practically the fillers tend to increase the dielectric loss of the composite as well. Employing a polymer with relatively high intrinsic K increases the effective K of the composite, because K of the polymer has a strong influence on the K of the final polymer composite. Also, fillers with high K and low loss should be selected to improve the properties of the overall composite. The challenge lies in designing a composite with less loss-inducing fillers to increase the effective K of the composite and finding a suitable polymer with high-K.

1.6 Research focus

This work focuses on the fabrication of nanodielectric capacitors for both embedded and discrete capacitor applications. The goal is to increase the effective dielectric constant of the composite formed by embedding Silver (Ag) nanoparticles in a Polyvinylpyrrolidone (PVP) host matrix. Here we report the effects of loading Ag nanoparticles in a PVP matrix in ethanol solvent and the control of the dielectric performance of this system by employing methods such as controlled dispersion, centrifugal separation of agglomerated nanoparticles, effect of multilayer layer dielectric films and various spinning regimes. The dielectric behaviors of the nanocomposites were studied systematically over a range of frequencies to determine the dependence of dielectric constant, dielectric loss tangent and dielectric strength on these parameters.

Finite element method (FEM)-based COMSOL Multiphysics software is used in this work to simulate the electrical properties of nanocomposites. Dielectric constant of the composite is calculated for different loading of Ag nanoparticles in 3D model. Percolation theory is used to estimate the theoretical effective dielectric constant of the nanocomposite films for different loadings of nanoparticles.

CHAPTER 2. BACKGROUND THEORY

2.1 Capacitors

A capacitor is a passive two-terminal electrical component used to store energy electro-statically in an electric field. Unlike batteries, they are designed to release their energy very quickly. All forms of capacitors contain at least two electrical conductors separated by an insulating region called dielectric. When there is a potential difference across the conductors, a static electric field develops across the dielectric, due to alignment of charges in the dielectric. This causes positive charge to collect on one plate and negative charge on the other plate. Energy of the capacitor is stored in the electrostatic field. The mechanism of working of a parallel plate capacitor in a circuit, including the alignment of charges in the dielectric material is shown in Figure 2.1.

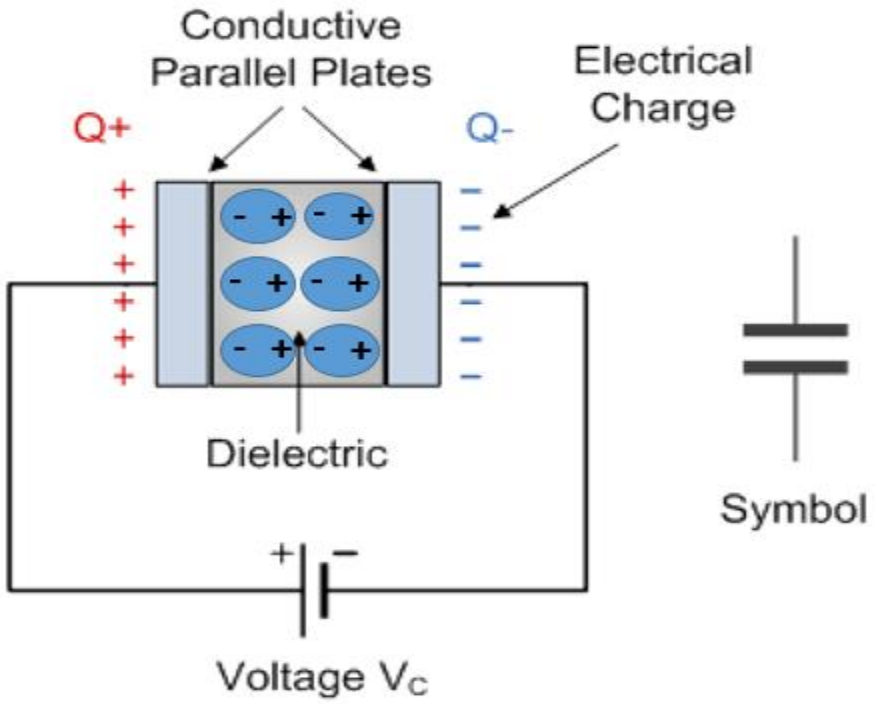

Figure 2.1 Mechanism of working of a capacitor.

The charge developed on the conductive plates is proportional to the voltage applied across the plates. Therefore, Q = C*V, where C is the constant of proportionality called Capacitance. Capacitance is a measure of electric charge stored in a capacitor.

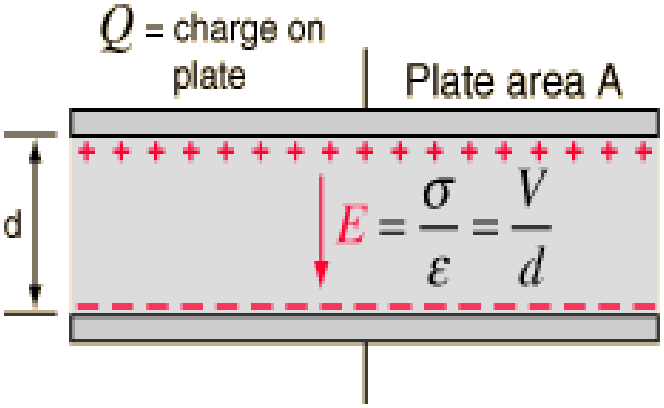

Figure 2.2 Parallel plate capacitor.

Consider a capacitor with 'A' as area of the parallel plates, d as distance between the plates as shown in Figure 2.2. A charge Q is developed on the plates when voltage V is applied across the plates. The electric field between the two parallel plates is given as E = $\frac{\sigma}{\varepsilon}$, where σ is charge density given as $\frac{Q}{A}$, and ε is permittivity of free space. The voltage difference between the two plates can be expressed in terms of the work done in moving a positive charge q from the positive to the negative plate, given as V = $\frac{Fd}{q} = E * d$. From the definition of capacitance, C = $\frac{Q}{V}$, we get C = $\frac{\sigma A}{Ed} = \frac{\varepsilon A}{d}$, which gives the expression for the capacitance of a parallel plate capacitor.

2.2 Effect of dielectric material in a capacitor

When a dielectric material (or a material with polar molecules) is placed in the medium between the parallel plates of a capacitor, the applied electric field will cause the charges in the material to align themselves relative to the field. This phenomenon is called dielectric polarization. The presence of the dielectric material reduces the effective

electric field, as shown in the Figure 2.3, and is given by the expression $E_{effective}$ = E - $E_{polarization} = \frac{\sigma}{K\varepsilon_0}$. The factor K by which the effective electric field is decreased by the

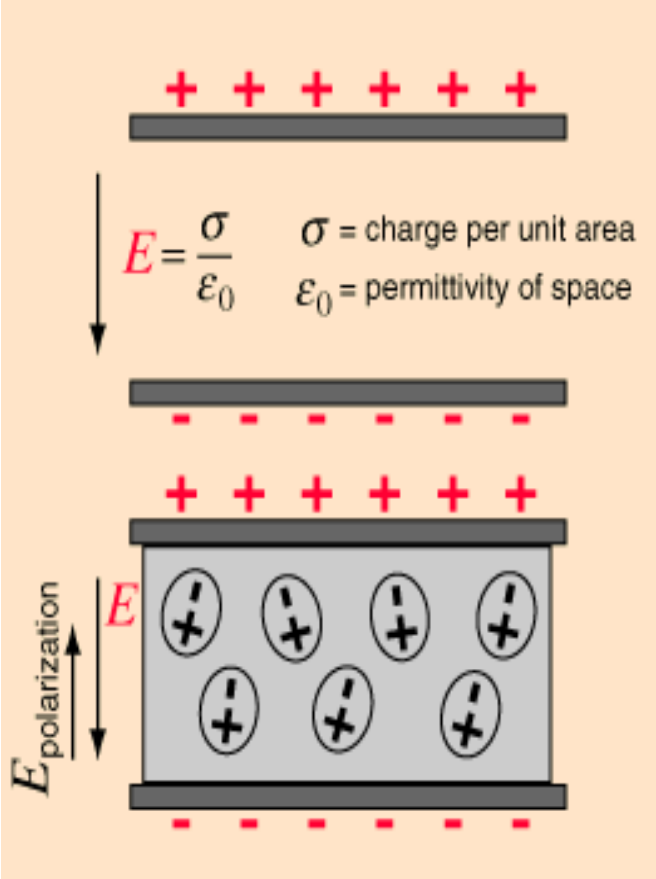

Figure 2.3 Effect of dielectric in a capacitor.

polarization of the dielectric is called the dielectric constant of the material. Now, the capacitance of the parallel plate capacitor is given as $C = \frac{\varepsilon_0 KA}{d}$, where ε_0 ($8.854*10^{-12}$ F/m) is the permittivity of free space and K (or ε_r or k) is the dielectric constant or permittivity of the material in between the plates. Thus, the capacitance increases by a factor of K, with the insertion of dielectric in between the plates. It is evident that the larger the dielectric constant, the larger the capacitance which can be realized in a given space. Therefore, materials of high dielectric constant are favored in practical design of embedded capacitors for miniaturization. The dielectric constant of a material is related

to its electric susceptibility by the relation $\chi_e = K - 1$. The electric susceptibility of a dielectric material is a measure of how easily it polarizes in response to an electric field.

The ability of the dielectric materials to store energy is attributed to the polarization, which can result in an increase in capacitance. There are several molecular mechanisms associated with this polarization, including electronic, ionic, molecular (dipole), and interfacial (space-charge) polarizations. For a given material, the sum of the contributions from each mechanism determines the net polarization P of the dielectric material, and is expressed as

$$P = P_{electronic} + P_{ionic} + P_{molecular} + P_{interfacial} \,. \quad (1)$$

Electronic polarization occurs in neutral atoms when the electric field displaces the positive nucleus with respect to the electrons around it. Magnitude of this mechanism is very small compared to other mechanisms, would result in low K, and can react to very high frequencies around 10^{15} Hz [7]. Ionic polarization involves the shifting of ionic species under the influence of electric field. This mechanism can result in very high K, up to several thousands, and is most prevalent at low frequencies. Molecular polarizations occurs in substances containing permanent dipole moments, and is observed at around 10^{11} to 10^{12} Hz. Interfacial polarization occurs in heterogeneous systems such as multi-component materials when translating charge carriers are accelerated by an applied field until they are impeded by and trapped at the physical barriers. It is observed at around 10^{-3} to 10^{3} Hz. The schematics of these polarization schemes are shown in Figure 2.4 and summarized in Table 2.1.

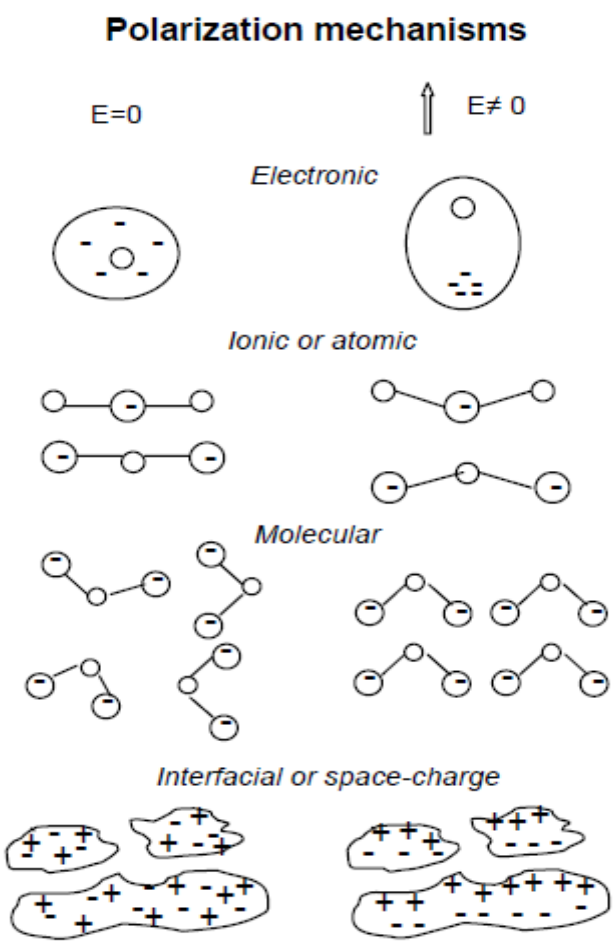

Figure 2.4 Schematics of major polarization mechanisms.

Table 2.1 Summary of polarization mechanisms.

Type of polarization	**Case where it is observed**	**Frequency range where it is predominant**	**Strength of polarization**
Electronic polarization	Neutral atoms	~ 10^{15} Hz	Very weak
Ionic polarization	Ionic species	10^{12} to 10^{13} Hz	Strong
Molecular polarization	Molecules with permanent dipole moment	~ 10^{11} to 10^{12} Hz	Weak
Interfacial polarization	Heterogeneous systems	10^{-3} to 10^{3} Hz	Very strong

2.3 Characteristics of suitable dielectric for embedded capacitor applications

2.3.1 High dielectric constant

A capacitor with an insulator of dielectric constant K can store K times more charge compared to a capacitor with air or vacuum as insulator. So, materials of high dielectric constant are favored in the design of embedded capacitors to achieve high energy density in a given space and further miniaturization. In an alternating field, dielectric constant can be expressed as

$$\varepsilon^* = \varepsilon' - j\varepsilon'' = \varepsilon_0\varepsilon_r - j\varepsilon'' \,, \tag{2}$$

where $\varepsilon'$is real permittivity, and $\varepsilon''$is imaginary permittivity. Real permittivity,ε' is directly related to the K of a material, and ε" is the dielectric loss factor of the material. Ideally, the dielectric constant should be constant with respect to frequency, temperature, voltage, and time. However, each polarization mechanism has a characteristic relaxation frequency. Therefore, K value of most of the materials show a dependence on the frequency because slower mechanisms fail to respond and contribute to the dielectric storage when the frequency becomes large. A spectrum of dielectric constant over a wide range of frequencies and the related polarization mechanisms associated with respective frequencies is shown in the Figure 2.5. The K values of dielectric materials can also vary with temperature, bias, impurity, and crystal structure by various extents depending on material types [5].

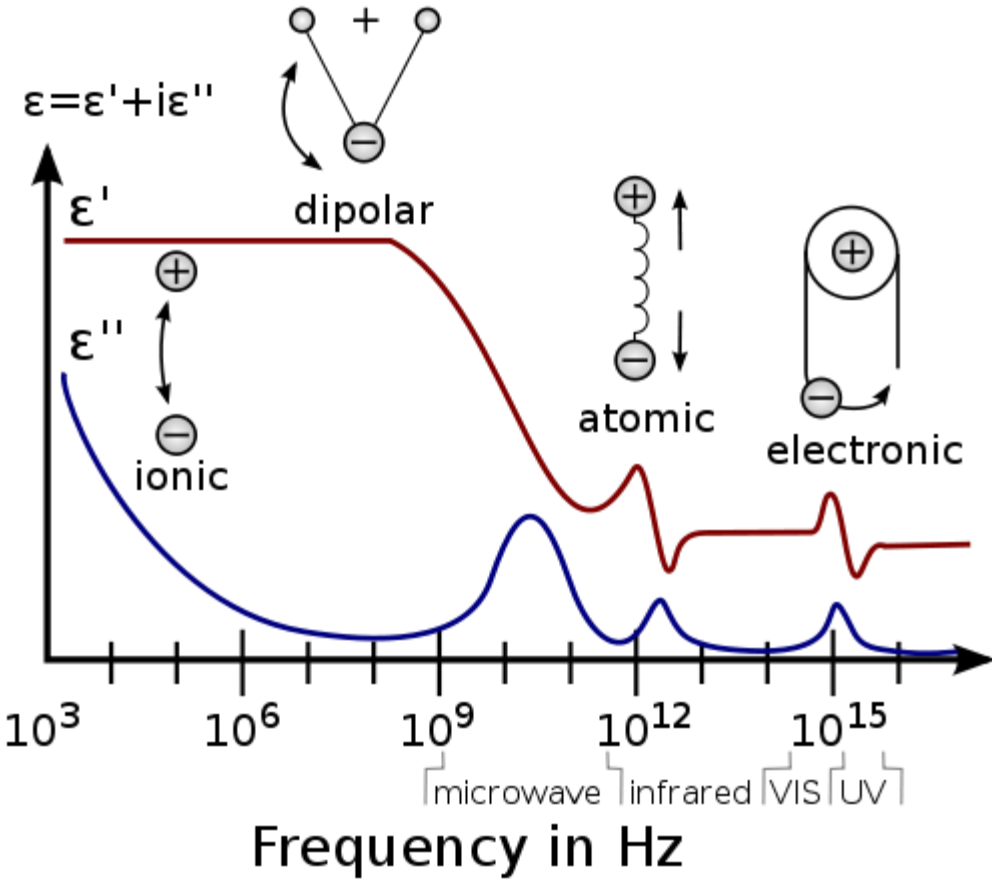

Figure 2.5 Spectrum of dielectric function showing associated polarization mechanisms.

2.3.2 Low dielectric loss

Dielectric loss is a material property of the dielectric and is a measure of energy loss of the dielectric during ac operation. Dielectric loss is a result of distortional, dipolar, interfacial and conduction losses. Dielectric loss is expressed as the loss tangent (tanδ) or Dissipation factor (Df), and is defined as

$$tan\delta = \frac{\varepsilon''}{\varepsilon'} + \frac{\sigma}{2\pi f \varepsilon'} \ , \qquad (3)$$

where ε', $\varepsilon''$are real and imaginary parts of complex permittivity, σ is electrical conductivity of the material and f is frequency. Energy loss (W) which is defined as the energy dissipated in a dielectric material is proportional to the loss tangent, and is expressed as

$$W \approx \pi \varepsilon' E^2 f \tan \delta, \quad (4)$$

where E is electric field strength and f is frequency [8]. Therefore, a low dielectric loss is preferred in order to reduce the energy dissipation and signal losses, particularly for high frequency applications. Generally, a dissipation factor under 0.1% is considered to be quite low and 5% is high [5].

2.3.3 High dielectric strength

Dielectric strength or breakdown voltage is a characteristic of an insulator that defines the maximum voltage difference that can be applied across the material before the insulator collapses and conducts. The breakdown voltage of a material is not a definite value because it is a form of failure and there is a statistical probability whether the material will fail at a given voltage. When a value is given it is usually the mean breakdown voltage of a large data sample. At any voltage higher than the breakdown voltage, the device can no longer function as a capacitor. Table 2.2 shows the dielectric properties of some materials along with specific capacitance, energy density and attainable thickness of those materials [5].

To sum up, the candidate dielectric materials for embedded capacitors should have high dielectric constant, low dissipation factor, high thermal stability and good dielectric properties over a broad frequency range. In addition to these traits, they should also be processible under low temperatures, have good adhesion to PCB layers and should have good mechanical properties which make them compatible with the low cost PCB industry.

Table 2.2. Characteristics of some dielectric materials.

Dielectric	Dielectric constant	Dissipation factor (%)	Thickness (μm)	Specific capacitance (nF/cm^2)	Energy Density at 5V ($\mu J/cm^2$)
Unfilled laminated polymer	4	0.1-1.5	25	0.14	0.002
Ferroelectric-filled polymer	50	<3	25	1.8	0.023
SiO_2	3.7	0.03	0.2	16	0.2
SiO	6	0.01	0.2	27	0.34
Al_2O_3	9	0.4-1	0.2	40	0.5
Ta_2O_5	24	0.2-1	0.2	110	1.4
TiO_2	40	2-5	0.2	180	2.3
$BaTiO_3$	~2000	5	1.0	1800	22

2.4 Overview of dielectric materials for embedded capacitors

In recent years, considerable attention has been devoted to the research and development of the candidate high-k materials to meet the stringent materials requirements of embedded capacitors. A wide variety of materials have been studied and evaluated for this application. Some of the materials are summarized in the following sections.

2.4.1 Ferroelectric ceramic/polymer composites

In ceramic/polymer composites, traditional ceramics such as $BaTiO_3$, $BaSrTiO_3$, and $PbZrTiO_3$, are modeled as fillers in a polymer matrix. These ceramic materials possess K (or k) value in several thousands. Most of the K values of polymer-ceramic

composites developed to date are below 100 at room temperature. By employing relatively high K polymer matrices, the K values of ceramic/polymer composites can be effectively enhanced because the K of polymer matrix shows very strong influence on the K of the final composites [9]. This is demonstrated in the works of X. Zhao and others. Poly(vinylidene fluoride-trifluoroethylene) (PVDF-TrFE)) copolymer, a class of relaxor ferroelectric, can have a relatively high room temperature K (~40) after irradiation treatment [10]. Bai et al. prepared $Pb(Mg_{1/3}Nb_{2/3})O_3$-$PbTiO_3$/P(VDF-TrFE) composites with K values above 200 at 10 kHz [9]. Rao et al. reported a lead magnesium niobate-lead titanate (PMN-PT, 900 nm)+$BaTiO_3$ (50 nm)/high-K epoxy system (effective K: 6.4) composite with k value about 150 at 10 kHz, in which ceramic filler loading as high as 85% by volume [11]. A major concern for ceramic/polymer composites is that the high filler loading of ceramic powders will lead to some technical barriers for real application in the organic substrate, including poor dispersion of the filler within the organic matrix, and poor adhesion of the dielectric layer to other layers in PCB.

2.4.2 All organic polymer composites

The composites fabricated by dispersing an organic filler material possessing very high dielectric constant in a polymer matrix can exhibit high-K as well. Zhang et al. used copper-phthalocyanine (CuPc) oligomer, a class of organic semiconductor materials with k as high as 10^5, as high-k filler and dispersed in P(VDF-TrFE) matrix. The composite showed a k of 225 and a loss factor of 0.4 at 1 Hz [12]. Wang et al. further chemically modified CuPc and bonded to P(VDF-TrFE) to improve the dispersion of CuPc in polymer matrix. Dielectric loss was reduced and dielectric dispersion over frequency was weakened for chemically modified CuPc/P(VDF-TrFE) composites [13]. A k value above

1000 (@ 1 kHz) has been achieved by Huang et al. in an all-polymer high-k percolative composite material, fabricated by a combination of conductive polyaniline (PANI) with a poly(vinylidene fluoride-trifluoroethylene-chlorotrifluoroethylene) [P(VDF-TrFECTFE)] terpolymer matrix (k > 50) [14]. Lu et al. reported a PANI/epoxy composite prepared by in-situ polymerization with a high dielectric constant close to 3000, a dielectric loss tangent less than 0.5 at room temperature and 10 kHz [15]. The possibility of all-organic composites as candidate high-k material for embedded capacitor requires further investigation and demonstration.

2.4.3 Conductive filler/polymer composites

Conductive filler/polymer composites, which are based on percolation theory, are an alternate approach to ceramic/polymer composites**.** Ultra-high k values have been calculated with conductive filler/polymer composites when the concentration of the conductive filler approaches the percolation threshold, explained by the relation

$$\frac{\varepsilon_{eff}}{\varepsilon_h} = |f - f_c|^{-s} , \tag{5}$$

where ε_{eff} is the dielectric constant of the composite, ε_h is the dielectric constant of the host polymer, s is scalar constant, f is the concentration and f_c is the percolation threshold concentration of the conductive filler within the polymer matrix [16]. The constant 's' is a scaling constant which depends on the material properties, microstructure and connectivity of the metal-insulator composite [47-50]. Thus, this percolative approach requires much lower volume concentration of the filler compared to traditional approach of high-k fillers in a polymer matrix. Various metal particles or other conductive fillers, such as silver (Ag), aluminum (Al), nickel (Ni), carbon black, have been used to prepare the polymer conductive filler composites or three-phase percolative composite systems.

High dielectric loss, low dielectric strength and narrow processing window are technical barriers for this category of materials because the highly conductive particles easily form a conductive path in the composite as the filler concentration approaches the percolation threshold.

2.5 Current trend in embedded capacitors

2.5.1 Nanocomposites

A nanocomposite (NC) is a multiphase solid material where one of the phases has at least one dimension which is less than 100 nanometers. These materials typically contain an inorganic component in an organic host or vice versa, or consist of two or more inorganic/organic phases in some combinatorial form with the constraint that at least one of the phases is in the nano-size dimensions. The mechanical, electrical, thermal, optical, electrochemical, catalytic properties of the nanocomposite will differ markedly from that of the component materials.

2.5.2 Nanofillers

Nanofillers are those fillers of sub 100 nm size in at least one dimension. The small size of the nanofillers gives rise to unique and excellent electrical, magnetic, optical, catalytic, mechanical, chemical or biological properties, such as surface plasmon resonance, coulomb blockade effect, plasmon absorption, super paramagnetism etc. Also, nanoparticles have a much higher surface area per unit volume than larger particles, and thus possess a much greater interface with their surroundings. Nano-sized particles are preferred for high-k dielectric composite materials because they could help achieve thinner dielectric films leading to a higher specific capacitance.

2.5.3. Processing of polymer nanocomposites

To utilize the unique optical, electrical and magnetic properties of nanoparticles for different applications, it is very important to understand, tailor and optimize their properties by controlling the size, shape, volume fraction, interface, degree of dispersion or aggregation. This is called processing of nanocomposites, and is one of the major limitations in the commercialization of nanocomposites. Processing of nanocomposites consists of controlled dispersion, making changes in the synthesis method, or modifying the interface of nanoparticles in the host polymer.

All the above mentioned processing techniques were tried in this work, and the dielectric behaviors of the nanocomposites were studied systematically over a range of frequencies to determine the dependence of dielectric constant, dielectric loss tangent and dielectric strength on these parameters.

CHAPTER 3. THEORETICAL MODELING AND SIMULATION

3.1 Drude-Lorentz model for dielectric function of size dependent nanoparticles

The theoretical complex dielectric function (ε) for a metal may be represented by the classical Drude free-electron model (or Drude model) in combination with the Lorentz oscillator model for the bound-electron [17]. The complex dielectric function for the Drude model is given by

$$\varepsilon_{free}(\omega) = 1 - \frac{\omega_{pf}^2}{\omega^2 + i\omega\gamma_f} \ , \tag{6}$$

with $\omega_{pf}^2 = \frac{N_f e^2}{\varepsilon_0 m_0}$, where ω_{pf} is the plasma frequency, $1/\gamma_f = \tau_f$ is the free electron scattering time or damping constant; N_f, e, m_0, are the free-electron density, charge, and effective mass respectively. It has been shown that the bulk dielectric function for metals is applicable for nanoparticles by introducing an altered damping constant that incorporate size effects [18]. As the particle size approaches the mean free path of electron in bulk metal, scattering at the particle surface becomes important and is modeled by modifying the damping constant and making it a function of particle size. The damping constant is given as

$$\frac{1}{\tau_f} = \frac{1}{\tau_0} + 2\,\frac{V_f}{d}\,, \tag{7}$$

where τ_0 is the scattering time in the bulk material, V_f denotes the Fermi velocity, and d is the particle diameter.

$$\frac{1}{\tau_0} = \gamma_0 = \frac{V_f}{l_b}\,, \tag{8}$$

where l_b is the bulk mean free path [19]. The Lorentz oscillator model for a bound electron used to describe an intraband transition yields the dielectric function

$$\varepsilon(\omega)_{bound} = \frac{\omega_{pb}^2}{\omega_0^2 - \omega^2 - i\omega\gamma_b}, \tag{9}$$

with $\omega_{pb}^2 = \frac{N_b e^2}{\varepsilon_0 m_0}$, where ω_0 is the bound-electron resonant frequency, $1/\gamma_b = \tau_b$ is the bound-electron decay time, and N_b is the bound electron density. The Drude model adequately describes the dielectric response for most metals below the threshold for interband electronic transitions. Above this threshold, which is predominant in noble metals, the dielectric response requires a combined Drude and Lorentz model [20], because the polarizabilities are additive, so

$$\varepsilon_{bulk}(\omega, d) = 1 - \frac{\omega_{pf}^2}{\omega^2 + i\omega\gamma_f} + \frac{\omega_{pb}^2}{\omega_0^2 - \omega^2 - i\omega\gamma_b}, \tag{10}$$

where $\varepsilon_{bulk}(\omega, d)$ is the size-dependent dielectric constant of a noble metal. Table 3.1 shows the values of all parameters used to calculate $\varepsilon_{bulk}(\omega, d)$ and their references.

Table 3.1 Parameters involved in calculation of the dielectric function of silver.

Parameter	**Symbol**	**Value**	**Reference**
Plasma frequency	ω_{pf}, ω_{pb}	$2.17*10^{15}$ Hz	28
Bound electron damping frequency	γ_b	$4.353*10^{12}$ Hz	31
Resonant frequency	ω_0	$0.27*10^{14}$ Hz	30
Drude relaxation frequency in bulk material	γ_0	$0.3225*10^{14}$ Hz	29,31
Fermi velocity	V_f	$1.38*10^6$ m/s	28
Mean free path	l_b	40 nm (at 100 ^{0}C)	28
Free electron density	N_f	$5.85*10^{22}$ /cc	28
Damping frequency	γ_f	$1.11*10^{14}$ Hz	From (7), at d=35 nm

3.2 Effective Medium Theories

The analysis of dielectric mixture systems, for instance, particles embedded in a host medium is a problem of enormous complexity if every single particle is considered individually. Alternatively, the resulting macroscopic material parameters of the mixture can be derived which describe the interaction between the composite material system and electromagnetic waves. To calculate this effective material parameter, effective medium theories (EMTs) can be employed [21]. EMTs are used to calculate the conductivity and dielectric constant of mixtures. EMT's are valid for spherical inclusions in the host medium and at low volume fractions [22]. Some of the common EMT's are tabulated as below,

Table 3.2 Some common EMTs and their expressions.

EMT	Expression
Maxwell model	$\varepsilon_{eff} = \varepsilon_h + 3f\frac{\varepsilon_i - \varepsilon_h}{\varepsilon_i + 2\varepsilon_h}\varepsilon_h$
Maxwell Garnett model	$\varepsilon_{eff} = \varepsilon_h\left[\frac{1 + 2f\left(\frac{\varepsilon_i - \varepsilon_h}{\varepsilon_i + 2\varepsilon_h}\right)}{1 - f\left(\frac{\varepsilon_i - \varepsilon_h}{\varepsilon_i + 2\varepsilon_h}\right)}\right]$
Asymmetric Bruggeman model	$\frac{\varepsilon_i - \varepsilon_{eff}}{\varepsilon_i - \varepsilon_h} = (1 - f)\left(\frac{\varepsilon_{eff}}{\varepsilon_h}\right)^{\frac{1}{3}}$

where ε_{eff} is the effective dielectric constant of the composite, ε_h is the dielectric constant of the host polymer, ε_i is the dielectric constant of filler material and f is the volume fraction of loading.

3.3 Percolation theory

Percolation theory takes into account the distribution of minor phase in the microstructure of the composite, which depends on its shape, size, and orientation. Percolation theory is significant when loading of minor phase of fillers reaches a critical

value; at this critical value, substantial changes take place in the physical and electrical properties of the system, sometimes on the order of more than a hundred times. This critical fraction of filler is called the percolation threshold, f_c.

For a metal filled conductor-insulator system, its large dielectric constant near critical filler loading can be explained by the percolation theory [23]. When the concentration of the metal is close to the percolation threshold, a large number of metal clusters will be formed. These metal clusters will act as the electrodes of capacitors when they are loaded in an external electrical potential. Now, the composite can be regarded as a "super capacitor network" with very large area and very small thickness [24]. According to the scaling theory, the dielectric constant of a percolation system should exhibit a power-law behavior [25], which can be expressed as

$$\frac{\varepsilon_{eff}}{\varepsilon_h} = |f - f_c|^{-s} , \tag{11}$$

where ε_{eff} is the effective dielectric constant, ε_h is the dielectric constant of the host material, f is the fraction of inclusions and f_c is the percolation threshold. Standard percolation theories on three-dimensional lattices assume that the percolation threshold is around 0.16 and critical exponent s is approximately unity.

3.4 Finite element modelling

Finite element method (FEM), often known as finite element analysis (FEA), is a numerical technique used to find approximate solutions of partial differential and integral equations of engineering and physics problems [26]. FEM is a method for solving an equation by approximating continuous quantities as a set of quantities at discrete points, often regularly spaced into a so-called grid or mesh. Since finite element methods can be adapted to problems of great complexity and unusual geometry, they are an extremely

powerful tool in the solution of important problems in heat transfer, fluid mechanics, and mechanical systems. Furthermore, the availability of fast and inexpensive computers allows phenomena which are intractable using analytic or mechanical methods to be modeled quickly and inexpensively using finite element methods.

FEM requires a problem to be defined in geometry and subdivided into a number of symmetrical identities, called mesh elements. The modeling of complex engineering systems involves designing, simulating, analyzing, post-processing, testing and fabricating [27]. Modeling and simulating techniques prove to be cost effective by prototyping and testing a product before it is actually manufactured.

There are generally two types of analysis that are used in industry: 2-D modeling, and 3-D modeling. While 2-D modeling conserves simplicity and allows the analysis to be run faster, it tends to yield less accurate results. 3-D modeling, however, produces more accurate results but are time consuming and require fast computing resources.

In practice, a finite element analysis usually consists of three principal steps:

1. Preprocessing: Here we construct a model of the physical entity to be analyzed, in which the geometry is divided into a number of discrete sub-regions called “elements," connected at discrete points called “nodes". These models can be extremely time consuming to prepare, and commercial software vendors vie with one another to have the most user-friendly graphical “preprocessor" to assist in this rather tedious chore.
2. Analysis: The physical properties are attributed to the materials, and boundary conditions are set for the physical model. Then, the model is solved for the solution using a system of linear or non-linear algebraic equations. Unknown

variables are approximated from known functions through the process of meshing, which applies to the small cells rather than to the entire geometry. Individual solutions from all the cells are integrated and approximated to get a solution for the entire geometry.

3. Post-processing: To show important trends and hot spots in the results, modern simulation software use graphical displays to visualize the results. A typical postprocessor display overlays colored contours representing hot spots or stress levels on the model.

In this work, COMSOL Multiphysics 4.2a simulation kit is used for analysis. The 3D space dimension type was selected for all the models. The physics model chosen was AC/DC analysis, and Electric currents module is selected. Frequency domain studies is then added, since it allows a frequency sweep to be conducted for different loadings of the nanofillers at different frequencies. The geometry of the capacitor model can be drawn either by using the built-in CAD module or by importing the CAD files. The geometries needed to simulate the composite nanodielectric environment are drawn in 3D model with varying filler fractions. Each of the loading fractions in all models is created as a separate file with an independent geometry. After the geometry is drawn, each section is assigned to the appropriate materials. The percolation theory is based on the difference in the properties of the insulator and the conductor materials, a difference that needs to be taken into account when simulating the 3D percolative composites. The outer block is designated as an insulating polymer PVP with an electrical conductivity (σ) of $5.5*10^{-8}$ S/m; the electrical conductivity of the spheres are set to a value of $63*10^{6}$ S/m, corresponding to silver (Ag). Another important characteristic for simulation is the

relative permittivity (dielectric constant) of each material, which is also attributed in the material properties. The dielectric constant of PVP is taken as 7, and the dielectric function of Ag is calculated for a range of frequencies using Equation 10.

After setting up the material characteristics, the next step is to simulate the model of a parallel-plate capacitor. This step can be done by setting proper boundary conditions in COMSOL Multiphysics. In 3D geometry, the top face is set to the port where input voltage is applied, while its opposite face is maintained at ground voltage. In the sub-domain settings, there is a provision to choose the basic governing equations. Equation $D = \varepsilon_0 \varepsilon_r E$ is chosen, as it is dependent on the electric field and the polarization of the composite. They are the major governing physics of metal-insulator nanodielectric composite capacitors. The boundary conditions for the remaining four sides of the geometry are maintained as electric insulation, which makes the model analogous to a parallel-plate capacitor with a voltage applied across its plates.

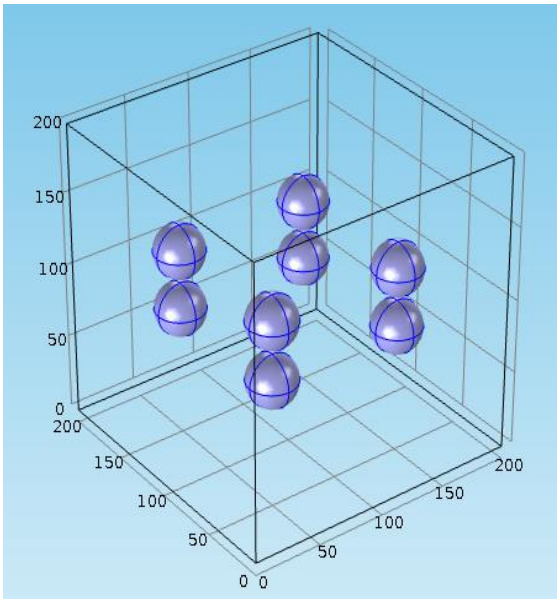

(a)

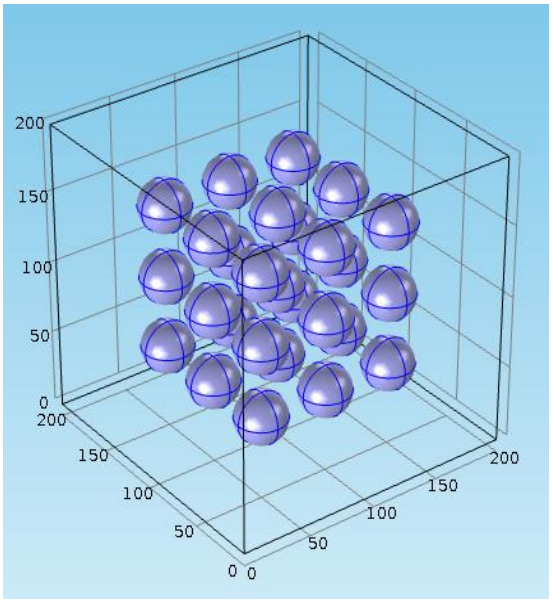

(b)

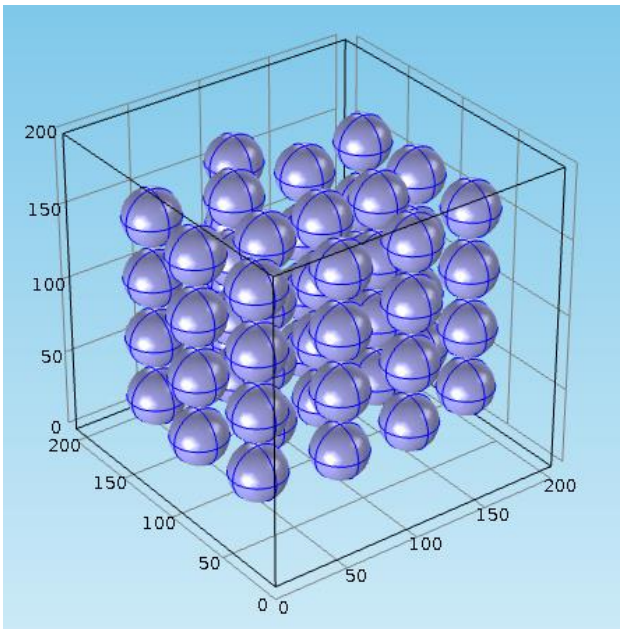

(c)

Figure 3.1 3D nanodielectric with (a) f=0.0225, (b) f=0.0757, and (c) f=0.157.

Figure 3.1 shows the geometrical setup of a 3D nanodielectric model containing spherical nanoparticles with a diameter of 35 nm in an enclosing PVP block of fixed volume. Figures 3.1 (a), (b), and (c) correspond to the three filler volume fractions of 0.0225, 0.0757, and 0.157 with 8, 27, and 56 nanoparticles respectively. The percolation threshold of spheres is 0.16, which is a universally accepted value known as Sher-Zaller invariant [36]. All the spheres in Figure 3.1 are at approximately equal spacing with one another in a block of fixed volume.

The final step in the simulation is to create small elements of the model by meshing. Meshing divides the geometry into small, discrete identities called elements, or cells. Unknown variables are approximated from known functions through the process of meshing, which applies to the small cells rather than to the entire geometry. Individual solutions from all the cells are integrated and approximated to get a solution for the entire geometry. Then, the model is solved to generate a three dimensional data set with

information on the model at steady state or time varying conditions. Post analysis allows us to generate slice and surface plots for surface polarization, electric potential and electric field etc.

CHAPTER 4. EXPERIMENTAL PROCEDURE

4.1 Materials

4.1.1 Silver nanoparticles

Nanoparticles are often defined as those particles with sizes in the range of 1-100 nm. Nanoparticle research is currently an area of intense scientific interest due to a wide variety of potential applications in biomedical, optical and electronic fields. The establishment of National Nanotechnology Initiative (NNI) in 2000 in the United States set the pace for nanotechnology research worldwide.

Silver nanoparticles have unique optical, electrical, and thermal properties and are being incorporated into products that range from photovoltaics to biological and chemical sensors. Conductive inks, pastes and fillers utilize silver nanoparticles for their high electrical conductivity, stability, and low sintering temperatures. Applications involving molecular diagnostics and photonic devices take advantage of the novel optical properties of these nanomaterials. In addition to these properties, nanoparticles exhibit unusual properties such as quantum confinement in semiconductor particles, surface plasmon resonance in some metal particles and super-paramagnetism in magnetic materials.

Polymer composite materials based on nanoparticles provide a potential solution to the demands of embedded capacitors in terms of the good processibility and mechanical properties of polymers combined with the unique electrical, magnetic or dielectric properties of nanoparticles. Nanoparticles are preferred for high-k dielectric composite materials because they could help achieve thinner dielectric films leading to a higher capacitance density.

4.1.2 PVP polymer

The polymer material chosen as host in the polymer nanocomposites should have fairly high dielectric constant since the intrinsic dielectric constant of the polymer plays a major role in determining the effective dielectric constant of the composite mixture. It should also have low dielectric loss and fairly high breakdown voltage for applications in embedded capacitors. A good combination of these properties in Polyvinylpyrrolidone (PVP) makes it a good choice as host for polymer nanocomposite materials for embedded capacitors.

A comparison of the properties of few dielectric films is shown in Table 4.1 [33]. From the table, it is clear that PVP has higher dielectric constant than the other polymers, while having low dissipation factor and a good breakdown voltage. It can also withstand relatively higher temperatures than the other polymers, which is useful during curing.

Table 4.1 General characteristics of a few dielectric films.

Polymer film	**Dielectric constant**	**Maximum temperature (°C)**	**Dielectric strength (V/µm)**	**Dissipation factor (%)**	**Energy density (J/cc)**
Polypropylene (PP)	2.2	105	640	<0.02	1-1.2
Polyester (PET)	3.3	125	570	<0.5	1-1.5
Polycarbonate (PC)	2.8	125	528	<0.15	0.5-1
Polyvinylidene fluoride (PVDF)	12	125	590	<1.8	2.4
Polyethylene naphthalate (PEN)	3.2	125	550	<0.15	1-1.5
Polyethylene sulfide (PPS)	3.0	200	550	<0.3	1-1.5
Polyvinylpyrrolidone (PVP)	7.0	300	300	<0.03	N.A

4.2 Instruments and characterization procedure

4.2.1 LCR meter

The capacitance and dissipation factors of the nanocomposites in this work with parallel plate prototype were measured by a portable LCR meter, DE-5000 from IET Labs Inc. and also by HP 4284A LCR meter. The capacitance measurements were made in the frequency range 100 Hz to 1MHz. The k values of the nanocomposites were calculated from capacitance measurements using the equation $C = \frac{\varepsilon_0 kA}{d}$, where ε_0 is permittivity of free space, A is the area of the parallel plate/contacts, d is the thickness of the dielectric.

4.2.2 SEM

A scanning electron microscope (SEM) is a type of electron microscope that produces images of a sample by scanning it with a focused beam of electrons. The electrons interact with atoms in the sample, producing various signals that can be detected and that contain information about the sample's surface topography and composition. The electron beam is generally scanned in a raster scan pattern, and the beam's position is combined with the detected signal to produce an image.

FEI XL-30FEG SEM was used to investigate the micro-structure of the high k nanocomposite materials. The SEM was used to study the dispersion uniformity of the filler particles, the size of the agglomerate, the thickness of the dielectric, and the connectivity between filler particles.

4.2.3 eBeam Evaporator

Electron Beam Physical Vapor Deposition or EBPVD is a form of physical vapor deposition in which a target anode is bombarded with an electron beam given off by a

charged tungsten filament under high vacuum. The electron beam causes atoms from the target to transform into the gaseous phase. These atoms then precipitate into solid form, coating everything in the vacuum chamber within line of sight with a thin layer of the anode material.

A schematic of eBeam chamber is as shown in the Figure 4.1. EBPVD is used in this work to deposit metal coatings on the dielectric films to make contacts for parallel plate capacitor prototype.

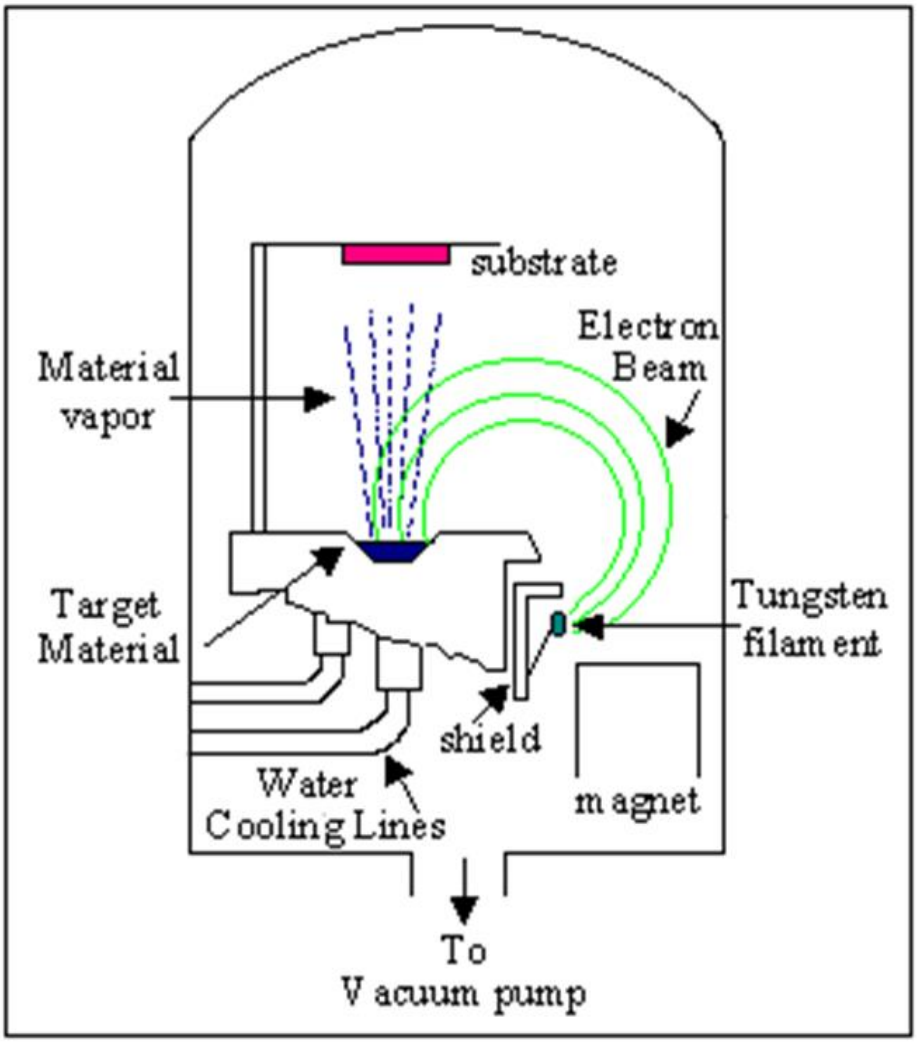

Figure 4.1 Schematic of eBeam PVD.

4.2.4 Centrifuge

A centrifuge is a piece of equipment, generally driven by an electric motor that puts an object in rotation around a fixed axis, applying a force perpendicular to the axis. The centrifuge works using the sedimentation principle, where the centripetal acceleration causes denser substances to separate out along the radial direction, and lighter objects tend to move to the top. Centrifuges are used in chemistry, biology, and biochemistry for isolating and separating suspensions. They usually comprise a rotor containing two, four, six, or many more numbered wells within which the samples, contained in centrifuge tubes, may be placed. Universal 320R benchtop centrifuge from Hettich Instruments was used in this work to separate suspensions and precipitate agglomerated nanoparticles.

4.2.5 I-V measurement setup

I-V measurements of the capacitor samples were obtained from a Keithley 6487 Picoammeter/voltage source controlled using the LabVIEW software to supply the input voltage and to read the output current. The leakage current was measured when a voltage was applied across the capacitor terminals. The voltage applied was increased until the current reached a value of 2.5 mA; this voltage was called the breakdown voltage. Input voltage was increased beyond the breakdown voltage to find a value of the voltage that the device can withstand before it forms a short circuit. The maximum voltage that can be applied using the Keithley 6487 was 500 V.

4.2.6 Surface Profilometer

In this research, the thicknesses of dielectric materials were measured by an Alpha-Step 200 Profilometer. Measurements were made electromechanically by moving

the sample beneath a diamond-tipped stylus. The sample beneath the stylus was moved according to the desired scan length, speed, and stylus force. Surface variations caused the stylus to be translated vertically and the instrument detected this motion.

4.2.7 Microtip sonicator

Sonication is the act of applying sound energy to agitate particles in a sample, for various purposes. Ultrasonic frequencies (>20 kHz) are usually used, leading to the process also being known as ultrasonication. Misonix Sonicator 3000 with microtip probe is used in this work to evenly distribute nanoparticles in solution, and also for speed dissolution, by breaking inter-molecular attractions in the solution.

4.3 Steps in experimental procedure

4.3.1 Preparation of Ag/PVP nanocomposite solution

The preparation of a uniformly dispersed nanocomposite solution is an important step in the fabrication of nanodielectric capacitors. The capacitance of the film coated using the Ag nanoparticles mixed in PVP solution depends on the concentration of the Ag nanoparticles in PVP solution. This concentration is called loading.

The Ag nanoparticles in powder form are mixed in the PVP solution to get a nanocomposite solution. The individual fractions of PVP and Ag nanoparticles are adjusted to get a desired loading value. The nanocomposite solution is thoroughly sonicated using a microtip sonicator for a duration of 5 minutes for speed dissolution and uniform distribution of nanoparticles.

4.3.2 Si wafer cleaning procedure

The PVP and nanoparticles mixture is spin-coated onto 1.5 cm x 1.5 cm size Si wafer, which acts as one of the terminals of the fabricated capacitors. Before the solution

mixture is spun, the Si wafer is cleaned to remove grease and other residual contaminants. The wafer is first blown with nitrogen gas to remove the dirt on the surface. Trichloroethylene (TCE), acetone, and methanol are used consecutively to clean the wafer. The Si wafer is immersed shining side up in a beaker of TCE solution. The beaker is now heated at 60 ^{0}C for 5 minutes. Then, the Si is removed from the solution and cleaned in the same way in acetone and methanol. Finally, the wafer is rinsed with deionized water before it is blown dry with nitrogen gas.

4.3.3 Spin coating the nanocomposite

Spin coating is a process used to apply uniform thin films on the top of flat substrates. When a polymer solution is placed on the wafer before spinning, or dropped during spinning, a thin film is formed on the substrate. The thickness and uniformity of this film depends on viscosity of the solution and the spinning speed, and the duration. To get a very thin film, a less-viscous solution is used at a higher spinning speed. Usually, the less-viscous solutions are formed by using a smaller amount of polymer in the solution.

The wafer is placed at the center on the top of the holder and held with mechanical suction. The nanocomposite solution is now deposited at the center of the wafer. The spinner is programmed so that it spins at 1000 rpm for 60 seconds. This spinning rate has been used, since it resulted in a uniform thin film of the nanocomposite solution in preliminary experiments.

After spin coating, the wafer is processed for permanent setting of the nanodielectric on the substrate. The wafer is cured or heated to remove moisture and form cross-linking of the polymer. A cross-link is a bond that links one polymer chain to

another. This leads to increased dielectric strength, since most of the solvent is evaporated and the only things left remaining are polymer and the nanoparticles, thus forming a very good dielectric. The post processing or curing is generally done by heating the sample. The polymer coated wafer is placed on a heater which is at an initial temperature of 45 ^{0}C, and then the temperature is gradually increased by 50 ^{0}C for every 5 minutes, till the temperature reached 225 ^{0}C. At 225 ^{0}C, the sample is heated for 5 minutes.

4.3.3.1 Difficulties with water based nanocomposite solutions

The selection of solvent for dispersion of Silver nanoparticles is an important step in the spin coating and fabrication process of capacitors. The viscosity of the solvent and the contact angle it makes with the surface of Silicon wafer determine the quality of the spin coat. Solvents with sufficient viscosity and which make low contact angles with Si wafer were selected in this work. The solvents should also be able to disperse the silver nanoparticles and dissolve the PVP polymer to make uniform dispersions. This necessitates the solvents to be polar with relatively high dielectric constant values. Solvents like ethanol, methanol, acetone, isopropanol, acetic acid, Dimethyl formamide (DMF), formic acid etc. meet the above requirements. Extensive measurements of contact angles of different solvents on hydrophilic and hydrophobic surfaces were made by Jaroslaw Dlerich et al. [38].

Water is a polar solvent and dissolves the PVP polymer. Though water is slightly viscous than solvents like ethanol and methanol; it makes a contact angle ranging from 50^0 to 54^0 on bare Silicon surface [37]. This value is higher than the contact angle made by the above mentioned solvents [38, 39]. This higher contact angle is a deterrent to the

sticking of the solution to the Si substrate during spinning**.** Figure 4.2 illustrates how the contact angle influences wetting of the surface.

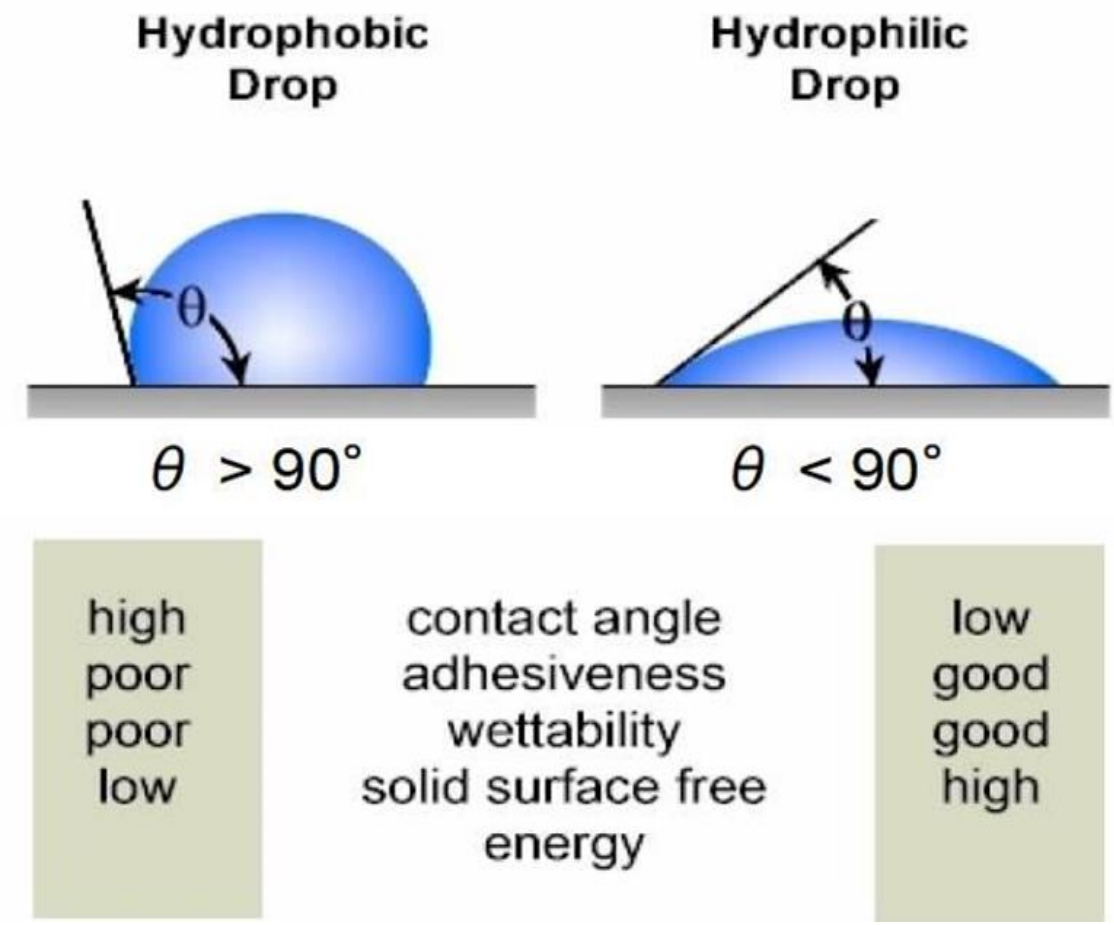

Figure 4.2 Effect of contact angle on the wetting of the surface.

In initial experiments, water was used as solvent to dissolve PVP polymer and the resulting nanocomposite solution was spin coated on Si wafer. The resulting film on Si wafer is non-uniform with varying thickness. Such a film when used to fabricate parallel plate capacitors gives capacitance with high degree of standard deviation across the sample. Figure 4.3 shows a thin film formed when water was used as solvent.

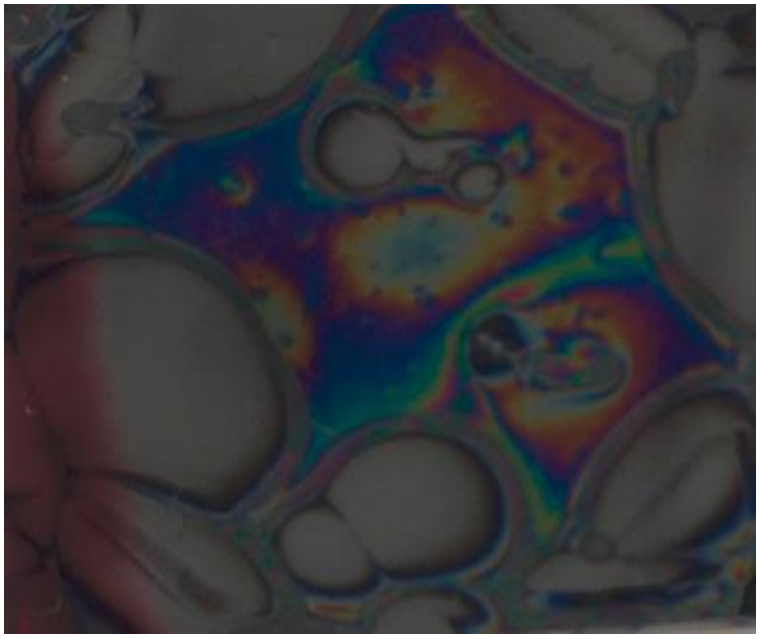

Figure 4.3 Non-uniform film formed when water is used as solvent.

4.3.3.2 Nanocomposite solution in ethanol

Ethanol is a polar solvent with a dielectric constant of 24.3. Ethanol dissolves PVP polymer and makes a low contact angle on Si compared to water. S. J. Spencer et al. made extensive measurements of contact angle on crystalline and mesoporous silicon [40]. It was found that the contact angle for ethanol–water mixtures was decreasing with increasing ethanol concentration for both untreated silicon and HF-dipped silicon up to an ethanol concentration of ~80%. At higher concentrations the contact angle approached zero.

4.3.4. Metal contact deposition

The metal contact deposition is the final stage of the parallel plate type capacitor slab fabrication technique. Aluminum metal is used in this case. The metal tip on the top of the dielectric, with highly doped Si wafer at the bottom, acts as a parallel plate capacitor. The metal contact deposition is done using eBeam evaporation.

4.4 Effect of the concentration/loading of the nanoparticles on the dielectric properties of the composite

Using ethanol as solvent, PVP and Ag nanoparticles are mixed and a uniformly dispersed nanocomposite solution is formed. The solution is sonicated using a microtip sonicator for 5 minutes for uniform distribution of nanoparticles. This solution is used for spin coating on the substrates. The resulting film was uniform and evenly distributed throughout the surface of the wafer. Nanocomposite solutions of various concentrations are made using ethanol as solvent and used to form nanodielectric films on gold coated Si wafer. Gold is coated prior on Si wafer to provide good electrical contact during measurement. Aluminum (Al) metal contacts are deposited on the nanodielectric films using eBeam evaporation technique. The resulting parallel plate capacitor prototypes were tested for dielectric properties. The results are summarized in the Figure 4.4, and show evidence of increase in capacitance as the loading of nanoparticles in the polymer was increased from 1% wt. to 4% wt. Beyond 4% wt., the capacitance values are found to be decreasing. This shows that the percolation threshold for Ag/PVP nanocomposite in ethanol solution is observed at 4% wt. loading of Ag fillers. The results are summarized in Table 4.2. The thickness of the dielectric films were measured using SEM, and the breakdown characteristics are analyzed from I-V measurements using Keithley 6487 setup controlled by LabVIEW software. The variation of K values among the capacitor samples are shown in Figure 4.5.

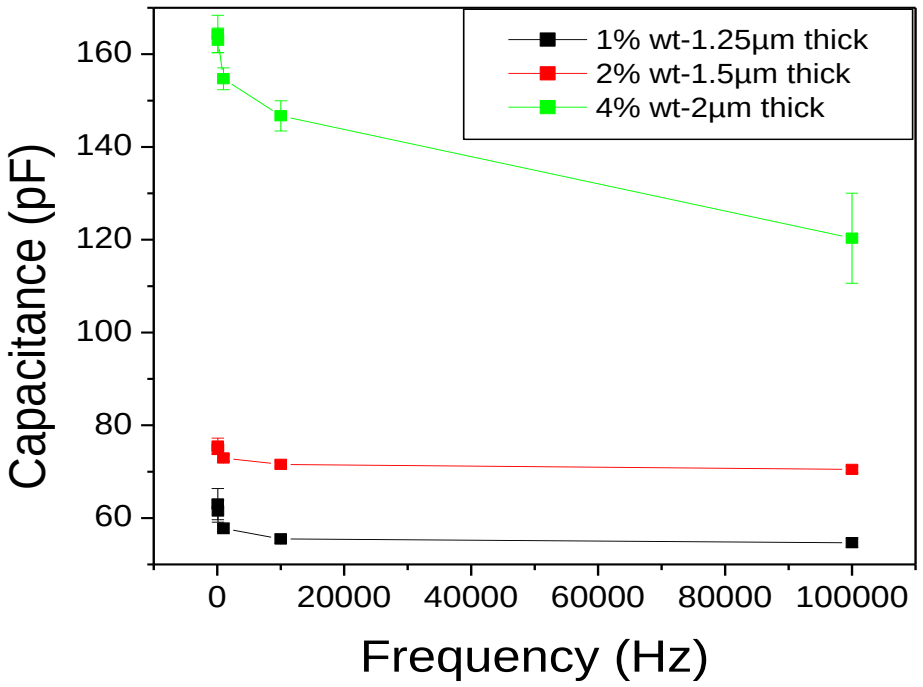

Figure 4.4 Variation of capacitance with concentration.

Table 4.2 Properties of nanodielectric films with Ag/PVP solution with varying concentration.

Loading concentration (% wt.)	**Capacitance at 100 Hz (pF)**	**Dissipation factor at 100 Hz**	**K value**	**Thickness of dielectric (µm)**
1	66	0.077	4.85	1.25
2	78	0.030	6.67	1.5
4	168	0.051	19.17	2
6	112	0.014	13.48	1.2
8	52	0.027	6.52	2.4
10	48	0.345	6.45	2.65

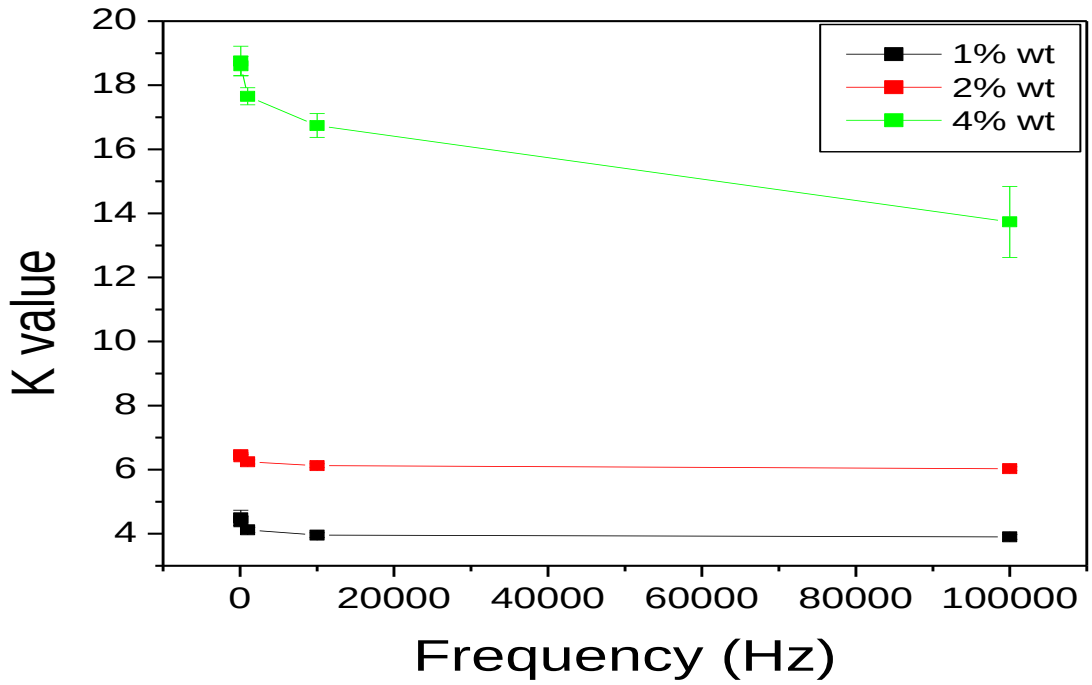

Figure 4.5 Variation of dielectric constant with concentration.

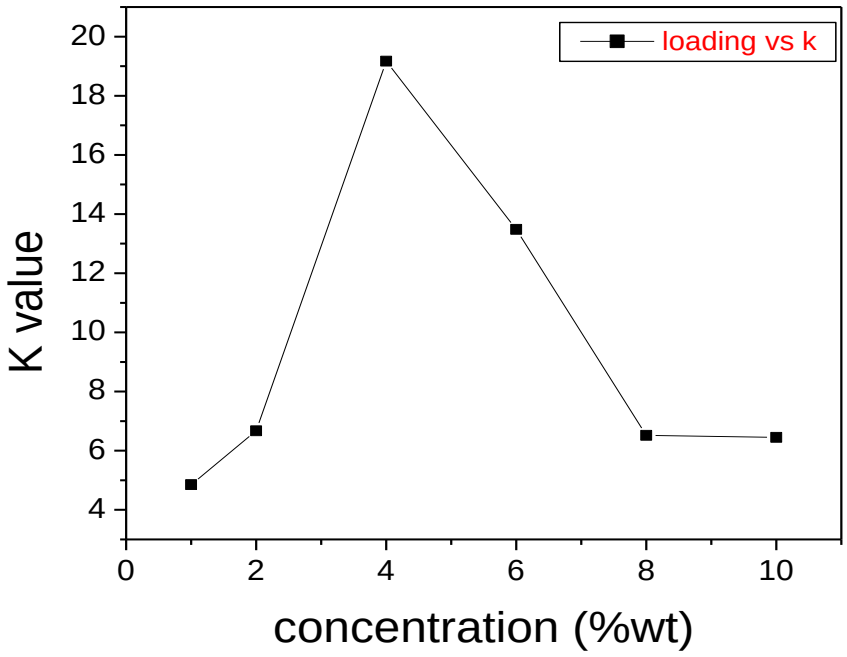

Figure 4.6 Observation of percolation threshold at 4% wt. using Ag/PVP nanocomposite in ethanol solution.

4.4.1 Thermal characterization of capacitors

For applications that require high operating temperatures such as those experienced in drilling of oil wells, thermal stability of passive capacitors becomes critical. Other applications also include high reliability applications such as avionics, automobiles and defense. Most commercial capacitors have a capacitance variation ranging from 1% to 30% with temperature, depending on the material of the capacitor and application field.

The fabricated nanodielectric capacitors were subjected to temperatures ranging from 50 ^{0}C to 175 ^{0}C, and resulting capacitance was measured using the LCR meter. The performance of various samples is summarized in Table 4.3, the plot in Figure 4.7 shows variation of capacitance with temperature.

Table 4.3 Thermal characteristics of capacitors of different concentrations.

Sample	**1% wt.**	**2% wt.**	**4% wt.**
Temperature (^{0}C)	**Cp (pF)**	**Cp (pF)**	**Cp (pF)**
50	65	77	124
75	63	72	116
100	60	69	87
125	58	61	74
150	57	60	72
175	55	57	63

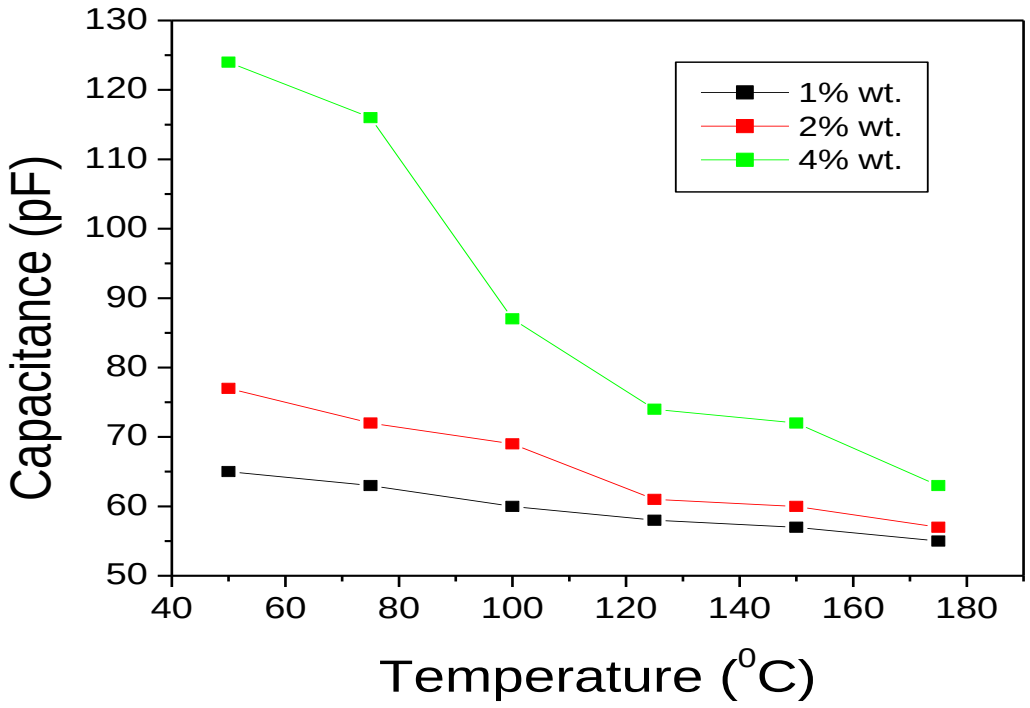

Figure 4.7 Variation of capacitance with temperature.

From Figure 4.7, it is observed that the capacitance reduced with increasing temperatures. The reduction of capacitance at 175 ^{0}C compared to room temperature for all the samples is summarized in Table 4.4. The higher loading fractions showed dramatic reduction in capacitance signifying that the temperature stability of the NC capacitors degraded with the nanoparticle fraction of loading.

Table 4.4 Reduction of capacitance over the temperature range.

Sample	**Reduction in Cp**
1% wt.	17%
2% wt.	27%
4% wt.	50%

4.4.2 Breakdown voltage test

Although ideally charge does not flow from one plate of the capacitor to the other, a small current called leakage current flows through the dielectric, slowly discharging the capacitor. This is due to defects and imperfections in the dielectric material causing charge transport pathways. Moreover, the higher the nanoparticle loading in the nanocomposite, the higher the chances for charge transport, through electron hoping or nanoparticle agglomeration. It is important to note that the leakage current in a capacitor is an important parameter in power supply circuits.

The leakage currents of capacitors are obtained by I-V measurements using a Keithley 6487 picoammeter/voltage source controlled with LabVIEW software. The voltage was applied across the capacitor terminals and the current was measured. The voltage was increased until the current reached a value of 2.5 mA. Unlike typical capacitors the leakage current did not show a drastic change with increasing voltage. Instead we observed a gradually increasing current, similar to a diode operation. Thus a voltage that gave a current of 100 μA or more was considered significant enough to classify it as the breakdown voltage. The leakage current characteristics of the capacitors are as shown in Figure 4.8. It is observed that the capacitors showed leakage currents in the range of 100 μA for lower voltages. The 1% wt. sample showed leakage currents in the range of 100 μA at 15 V, while the 2%, 4% wt. samples showed same leakage current around 8 V. Thus based on our definition of breakdown voltage, the lower fraction of loading NC capacitors gave a higher breakdown voltage as expected. For the 1% wt. sample, the leakage current reached a maximum of 2.5 mA at 35 V, whereas for 2% wt. sample it was reached at 28 V, and for 4% wt. sample it was reached at 30 V.

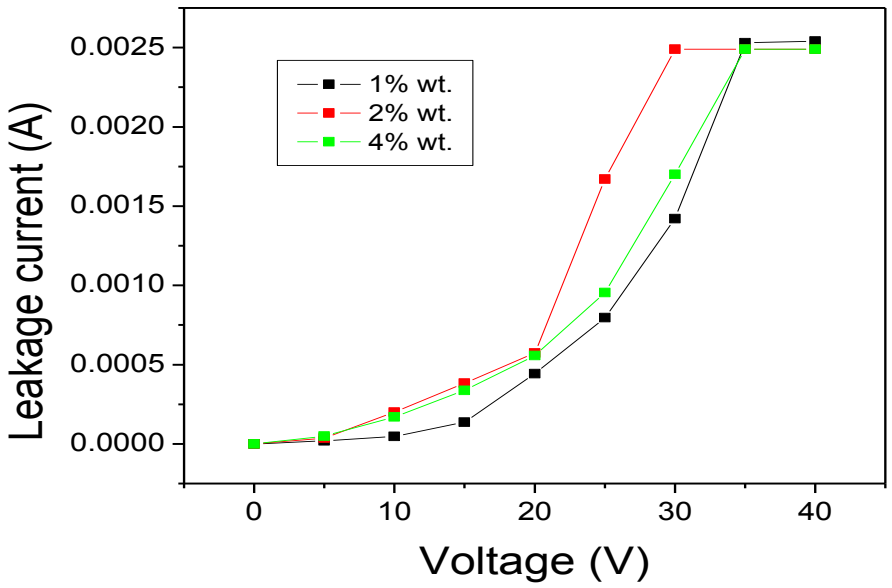

Figure 4.8 Leakage currents in capacitor samples.

4.5 Effect of distribution of nanoparticles on the dielectric properties of the composite

The distribution of nanoparticles is an important factor which determines the dielectric and electrical properties of nanodielectric capacitors [41]. It has been reported that poor dispersibility of nanoparticles might affect the dielectric and electrical properties [42-44]. Agglomeration of metal nanoparticles in the polymer film forms a conducting path which shorts the contacts and leads to catastrophic failure of the device. There are many doubts regarding as to how dispersibility of nanoparticles influences the specific properties of nanocomposites and what degree of dispersion is necessary to obtain excellent characteristics of the nanocomposite. Thus, there is a need to study the effect of dispersibility of nanoparticles on the dielectric properties of the nanocomposite.

Centrifugal force is used in this study to see the effect of distribution of nanoparticles on the dielectric properties of the composite. Centrifugal force separates

agglomerates from nanoparticles by precipitation. In this study, a 20% wt. ratio of Ag nanoparticles to PVP polymer in ethanol solution was prepared. Such a high concentration of solution was used since higher concentration solution has higher chances of agglomeration of nanoparticles. For the control of dispersibility, centrifugal force was used for different time durations and nanodielectric capacitors were fabricated from each of the solutions. Then, the dielectric properties like capacitance and dissipation factors were studied in each case. The results are shown in Figure 4.9. From the Figure 4.9, it is observed that while there is little or no improvement between 20 minute and 10 minute centrifuged samples, there is 12.6% improvement in capacitance between 40 minute and 10 minute centrifuged samples. Centrifugation times for even longer durations showed no improvements in our study. This is due to precipitation of all agglomerates and there are no more clusters of nanoparticles in the solution. The various dielectric properties are summarized in Table 4.5.

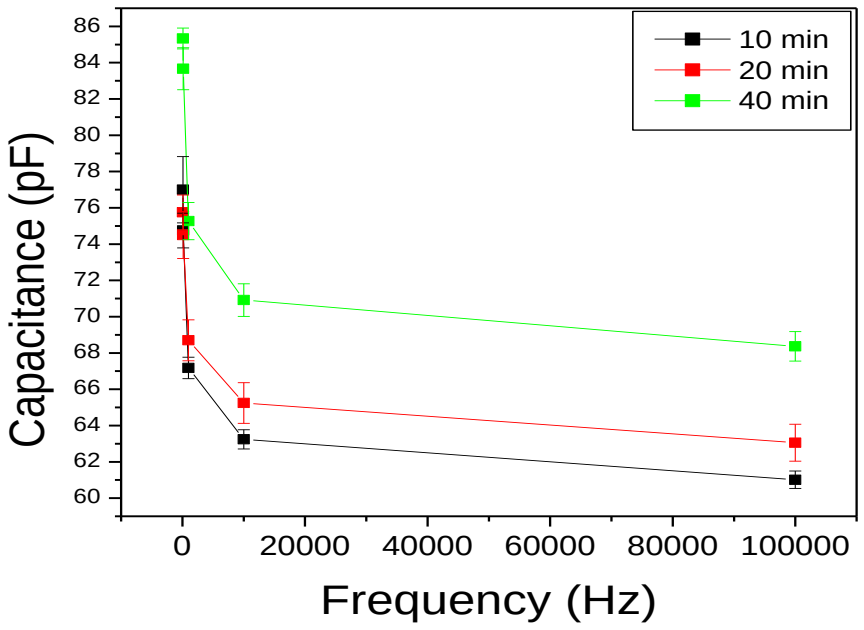

Figure 4.9 Variation of capacitance with centrifugation time.

Table 4.5 Dielectric properties of samples with different centrifugation duration.

Centrifugation time (min.)	Capacitance (Cp) at 10 kHz (pF)	Improvement in Cp compared to 10 min.	DF at 100 kHz	Thickness of dielectric (µm)	K value
10	63.24	-	0.032	3	10.825
20	65.254	3%	0.028	2.74	10.20
40	70.91	12.6%	0.033	3	12.13

4.5.1 Thermal characterization of capacitors

The results of the temperature tests on these capacitor samples are shown in Figure 4.10. As in the previous case, the capacitors showed degradation in capacitance at high temperatures. The reduction of capacitance of the respective samples is tabulated in Table 4.6. However, the degradation observed in these samples was lower than the previous capacitors of various concentrations.

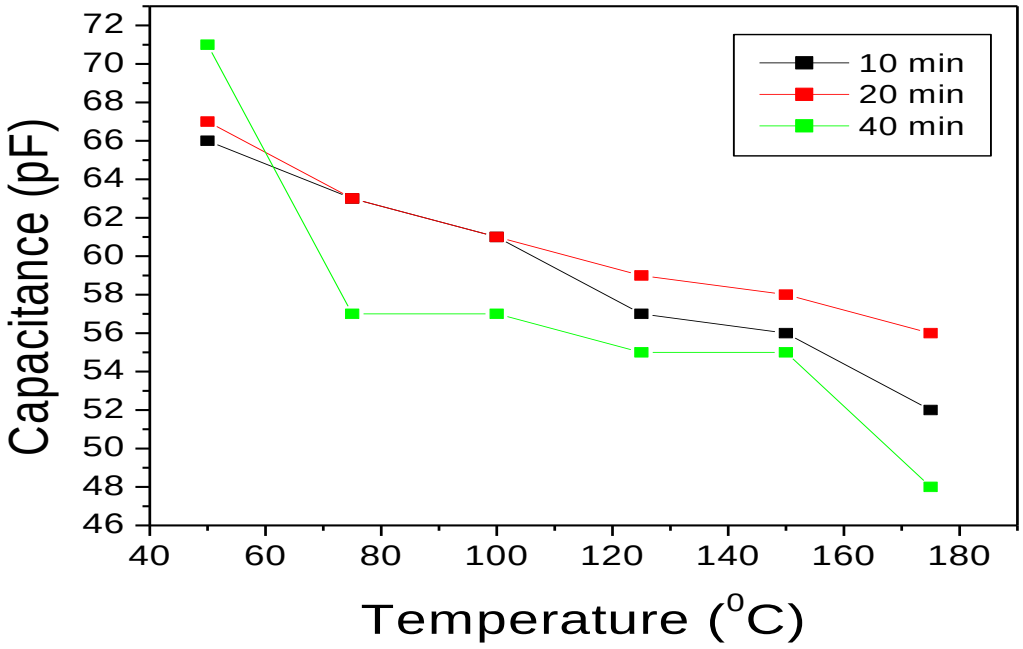

Figure 4.10 Thermal characteristics of centrifuged samples.

Table 4.6 Reduction of capacitance in centrifuged samples.

Sample	Reduction in Cp
10 min.	33%
20 min.	26%
40 min.	44%

4.5.2 Breakdown voltage test

The leakage current characteristics on these samples are as shown by the I-V curves in Figure 4.11. These capacitors showed much lower leakage currents in the range of 10^{-8} A in the entire 0-500 voltage range. It was difficult to determine the breakdown voltage of these capacitors, since the currents measured were very low. Moreover, at the time of testing we did not have a voltage source exceeding 500 V indicating that the dielectric strength of these capacitors will be greater than 166.67 V/µm for 3 µm thick dielectric. It is safe then to assume that the capacitors formed by the centrifugation process have superior performance compared to those prepared earlier.

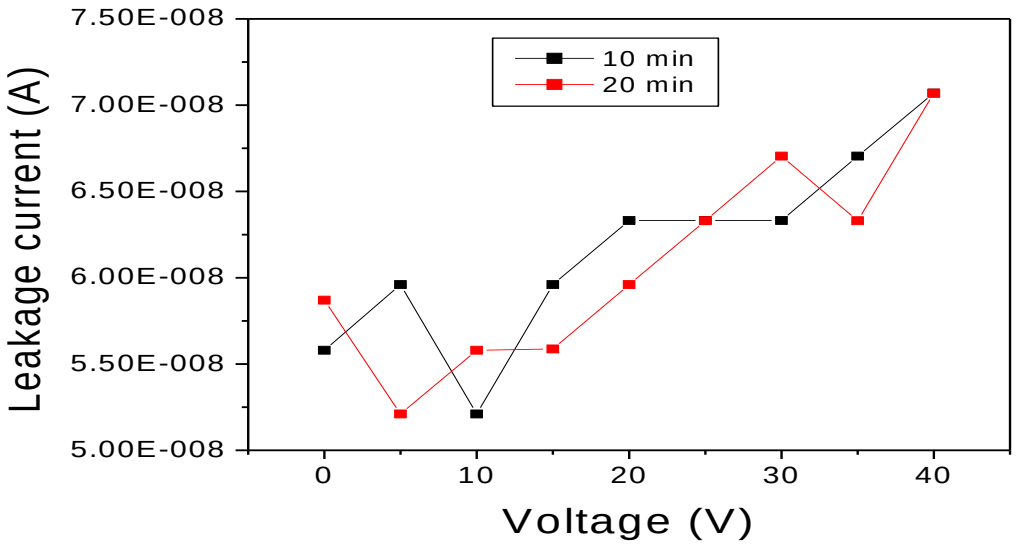

Figure 4.11 Leakage currents of centrifuged capacitor samples.

4.6 Control of dielectric properties of high k-composite by employing two different layers of dielectric

The composition of the dielectric, and its interface to the underlying substrate is an important factor in determining the dielectric and electrical properties of the capacitor. Deepak studied the properties of dielectric films formed from Ag nanoparticles in PVP polymer using water as a solvent [45]. He reported a dielectric constant of 40.67 using 0.04% wt. loading of nanoparticles in polymer, using ozone treatment to the Si substrate. Those dielectric films had non-uniform distribution, lacked uniformity, and had varying thickness due to high contact angle of water with Si surface. Moreover, we believe that ozone treatment of the silicon wafer forms a silicon dioxide layer on the surface which interferes with the bulk dielectric constant measurements of the polymer composite. To better exploit that works' dielectric properties and also achieve uniform films with homogenous thickness, a two layer dielectric model is conceived in this work. The realized two layer dielectric model is as shown in the Figure 4.12.

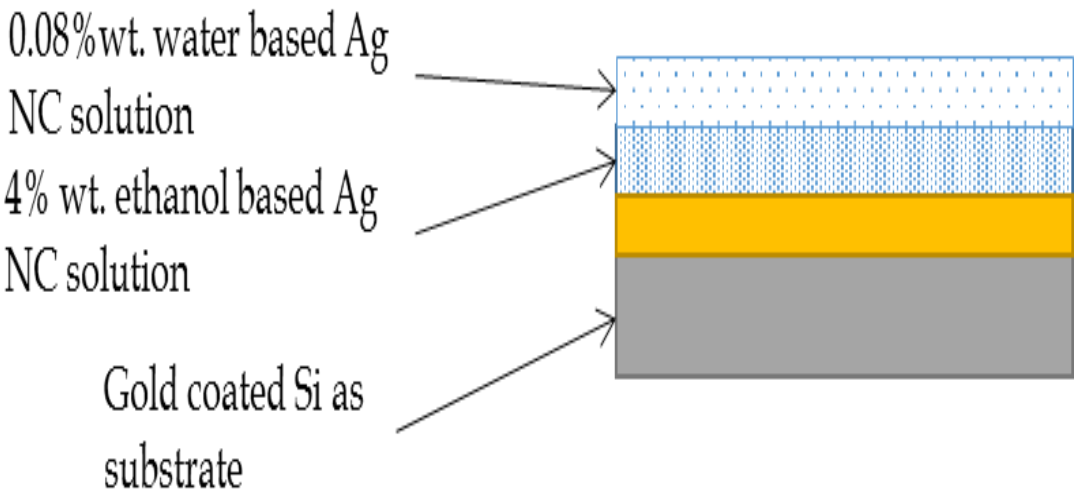

Figure 4.12 Two layer dielectric model on substrate.

A 4% wt. ethanol based NC solution which sticks well to the Si substrate is used as the first layer. It is spun at 5000 rpm for 60 seconds. This gives a uniform film due to better wetting properties on Si, and leaves a surface that allows better wettability for the water based NC solution. Then, 0.08% wt. water based Ag NC solution is spin coated onto the first layer at 1000 rpm for 60 seconds. The dielectric is cured, metal contacts are deposited, and the capacitor characteristics are measured. The results of this prototype are summarized in Table 4.7.

These two layer dielectric capacitors showed better frequency response characteristics compared to the 4% wt. loading capacitor samples discussed in Section 4.4. The regular 4% wt. capacitor samples discussed in Section 4.4 showed reduction in capacitance from 168 pF to 120.4 pF over the frequency range 100 Hz to 100 kHz, a

Table 4.7 Dielectric properties of two layer dielectric model capacitor.

Frequency (Hz)	**Cp (pF)**	**DF**	**K value**
100	78	0.008	10.68
120	78	0.005	10.68
1k	77.5	0.002	10.61
10k	77.16	0.001	10.56
100k	77.02	0.001	10.54

change in capacitance of 28.3% (refer Figure 4.4). But, the double layer dielectric capacitor samples showed very little change in capacitance from 78 pF to 77.02 pF over 100 Hz-100 kHz frequency range, a reduction of only 1-3%. Also, the dissipation factors of these double layer dielectric model capacitors are very low compared to the regular

single layer dielectric types (compare Table 4.2 and Table 4.7). The breakdown voltage of these samples is observed at 260 V, so the dielectric strength is 108.33 V/μm for a 2.4 μm thickness of dielectric.

4.7 Implementation of parallel connection of capacitors and investigate the charge storage and dielectric properties of the nanocomposite

Capacitors being one of the standard components in electrical circuits; complicated connections of capacitors often occur in practical circuits. So, it is important to find the equivalent capacitance of such combinations and understand how those combinations affect the charge storage and dielectric properties.

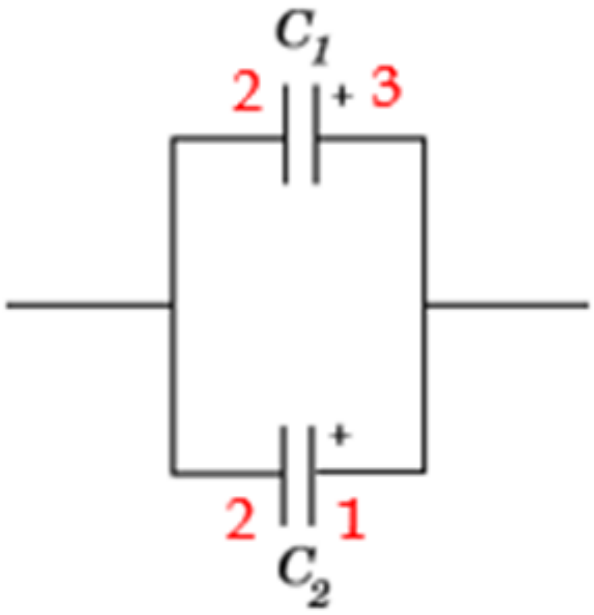

Figure 4.13 Parallel connection of capacitors.

For the parallel combination of capacitors as shown in Figure 4.13, the total charge is divided between the capacitors and the potential difference across the plates is the same. The labels 1, 2, 3 and 4 represent the plates of the capacitor and correspond to

the respective metal contacts labelled in Figure 4.14. The equivalent capacitance of the pair of capacitors is given by $C_{eq} = \frac{Q}{V} = \frac{Q_1 + Q_2}{V} = \frac{Q_1}{V} + \frac{Q_2}{V}$, giving $C_{eq} = C_1 + C_2$. If 'n' capacitors are connected in parallel, the equivalent capacitance is given as $C_{eq} = \Sigma_{i=1}^{n} C_i$. This property of parallel connection of capacitors is used to store large amount of charge and supply huge pulses of current for many pulsed power applications.

In this work, a parallel connection of capacitors was achieved based on the design as shown in the Figure 4.14. Metal contacts were deposited on dielectric layer and the dielectric layer was wiped using acetone at specific areas (or scratched from the surface) to form electrical connection between alternate metal contacts. The dielectric was cured before depositing metal contacts. Thus, parallel connection of capacitors was achieved.

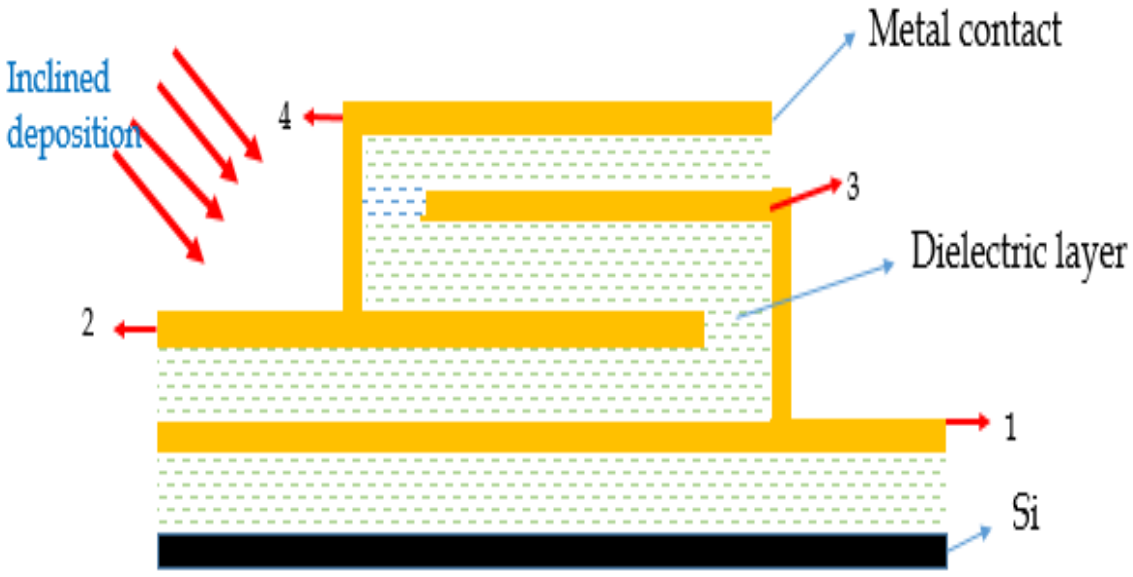

Figure 4.14 Design of parallel connection of capacitors.

A special mask was designed for this purpose to deposit metal contacts and to enable overlap of contacts for parallel connection as shown in Figure 4.15. The mask was flipped during subsequent metal depositions and it was ascertained that there was some

offset from the previous metal contact. This is to provide electrical contacts during measurement. Alumina was used as substrate for this design because it serves as an excellent electrical insulator and has high Mohs hardness value of 9. A 4% wt. Ag NC solution was used for spin coating on the substrate. The fabricated parallel connection of capacitors on Sapphire is shown in Figure 4.16. The increase in capacitance was observed after the design was completed. The results are summarized in Table 4.8.

The increase in capacitance is observed in the graph shown in the Figure 4.17. The thickness measurements were performed on the samples after each spin coat, and the k value was calculated. The k value for the capacitor was found to be 19.99 at 10 kHz, after measuring the thickness to be 1.4 µm. More than two fold improvement in capacitance is observed with the parallel connection.

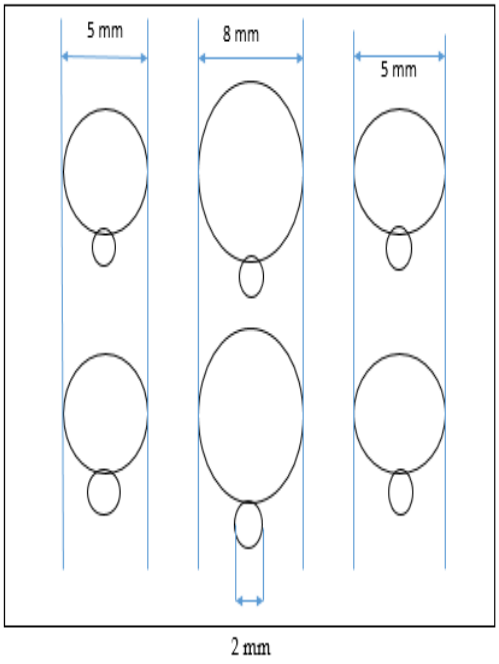

Figure 4.15 Mask design for parallel connection.

Figure 4.16 Parallel connection of capacitors.

Table 4.8 Results for parallel connection of capacitors.

Frequency (Hz)	Single capacitor-right contact		Parallel connection-right contact	
	Capacitance (pF)	**DF**	**Capacitance (pF)**	**DF**
100	1318	0.101	3463	0.818
120	1310	0.120	3390	0.72
1000	1242	0.05	2760	0.23
10000	1196	0.075	2480	0.212
100000	1168	0.23	2180	0.163

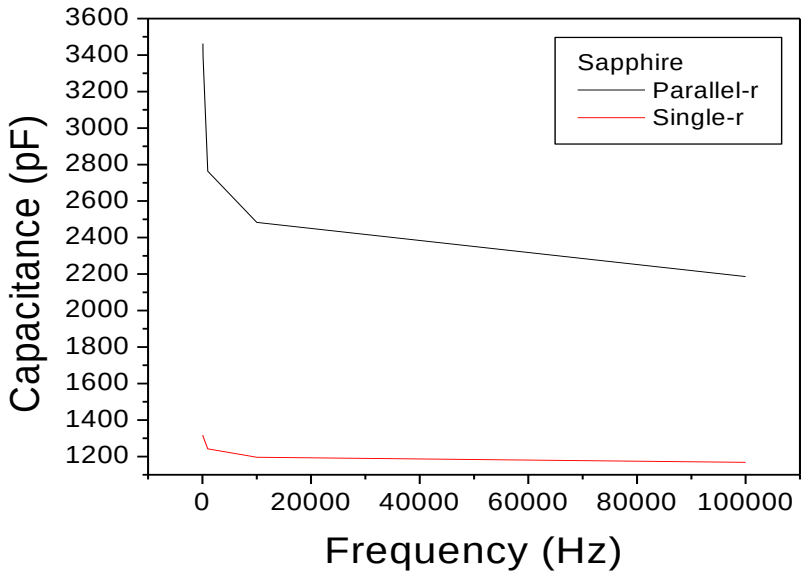

Figure 4.17 Parallel connection of capacitors on sapphire substrate.

CHAPTER 5. RESULTS AND DISCUSSION

5.1 Percolation theory predictions

The technique of preparing percolative composites to increase the dielectric constant of the polymer-based capacitors greatly depends on the concentration of the nanofiller. Aforementioned, the effective dielectric constant of the composites can be increased dramatically when the loading of the nanofillers is in the vicinity of the percolation threshold. As per percolation theory, the dielectric constant of the PVP matrix was predicted to be over a thousand times higher when the loading of the nanoparticle approached the percolation threshold (Figure 5.1).

Percolation theory, unlike EMTs, considers the metal/insulator nature of the Ag/PVP composites. According to percolation theory, a super capacitor network is formed at the percolation threshold, because of the difference in conductivities of the metal and insulator in the composite. This difference is taken into account by percolation theory, which predicts an increase in the effective dielectric constant at the percolation threshold. The effective dielectric constant calculation in this work, therefore, is predicted accurately by the percolation theory. The COMSOL Multiphysics simulations showed an increase in the polarization of the 3D composites when the loading of nanoparticles is near the percolation threshold. Near the percolation threshold of 0.16, the effective dielectric constant for 3D composites of Ag nanoparticles in PVP is calculated as 7000, which is a 1000 times increase as compared to the dielectric constant of PVP. The accuracy and how high the effective dielectric constant can go, depends on how precisely we could prepare the nanocomposite solution close to the percolation threshold of 0.16 without agglomeration.

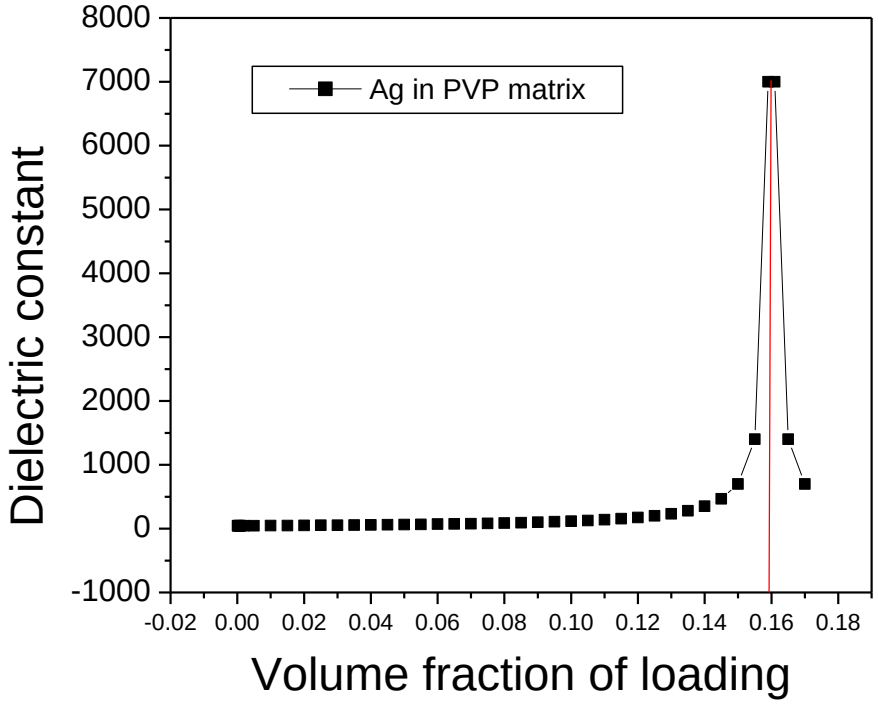

Figure 5.1 Graph plotted between the dielectric constant vs. volume fraction of filler.

Figure 5.1 is a plot between the loading of nanofillers and the dielectric constant of the composite calculated using Equation 5 (or Equation 11). It can be inferred from the figure that the dielectric constant of the composite increases gradually with an increase in the loading of nanofillers and reaches a maximum at the percolation threshold. At zero loading of nanofillers, the dielectric constant of the composite is the same as that of the polymer. As the loading approaches the critical value of the percolation threshold, there is a significant increase in the dielectric constant of the composite. If the loading of nanofillers is increased beyond the percolation threshold, the composite becomes conductive in nature, which leads to a rapid fall in the dielectric constant. The maximum K value that can be achieved depends on how precisely we could prepare the

nanocomposite solution close to the percolation threshold of 0.16 without compromising on agglomeration.

5.2 COMSOL modeling results

The parallel plate capacitors were modeled with Ag nanoparticles embedded in PVP dielectric medium using COMSOL Multiphysics simulations. Electric field generation and development of polarization patterns were studied. Three loadings of nanoparticles are studied and compared to understand the influence of change in the concentration of nanoparticles.

The dielectric constant of the material is directly related to the amount of polarization it undergoes in presence of an electric field. Thus, the surface polarization mechanisms are studied in the simulation to give an idea of the overall dielectric constant in each case and compared with different scenarios.

5.2.1 Effect of shape of the nanoparticles on the Surface polarization

Nanoparticles are commercially available in shapes such as spheres and rods. But, various other shapes such as nanocubes [34], fibers, cups and flakes can also be synthesized by using different materials during synthesis, such as miscellar emulsions or anodized aluminum pores [35]. The study of fine particles is called micromeritics. The knowledge and control of the size, shape and surface area of particles is of importance in pharmaceuticals and materials science.

Using the procedure for creating a model of parallel plate capacitor in 3D, as described in Section 3.4, geometries are drawn for capacitors with fillers in the shapes of spheres, cylinders and ellipsoids respectively. The volume of all the shapes is kept constant at a particular fraction of loading. In this way, we could know which shape of

the nanoparticles gives high polarization at a particular loading. The surface polarization plots are generated in each case. Observe that the number of nanoparticles (n=13) is the same for all the models because the volume of each nanoparticle is kept constant.

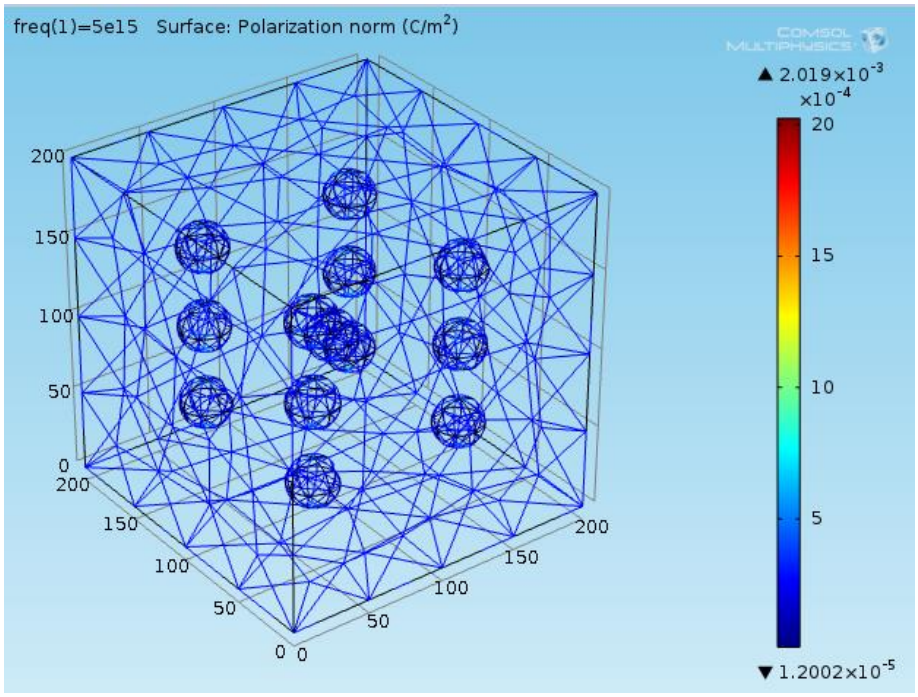

Figure 5.2 a) Surface polarization for spherical nanoparticles for f = 0.0225.

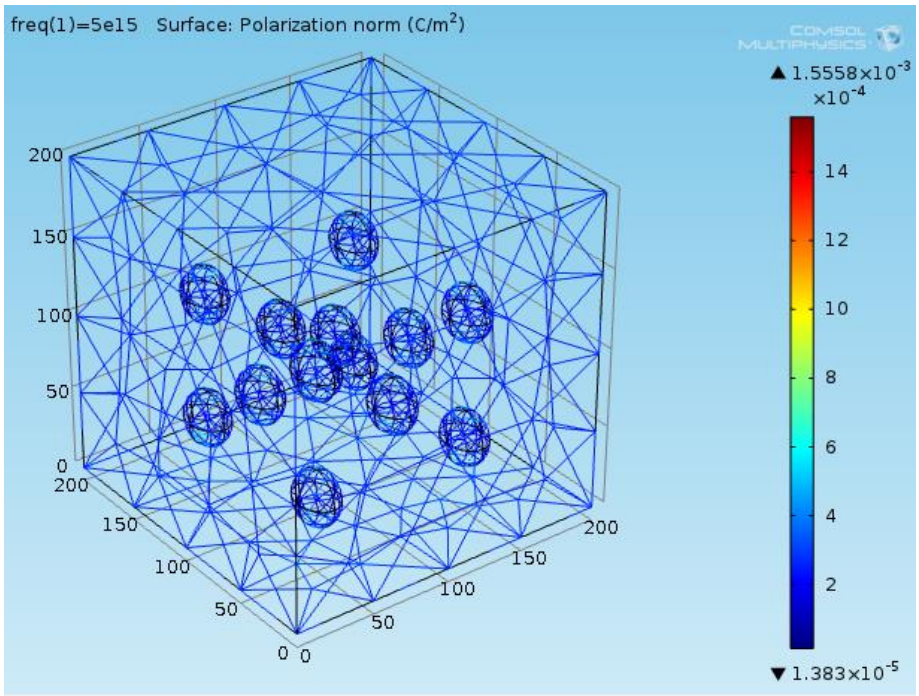

Figure 5.2 b) Surface polarization for ellipsoidal nanoparticles for f = 0.0225.

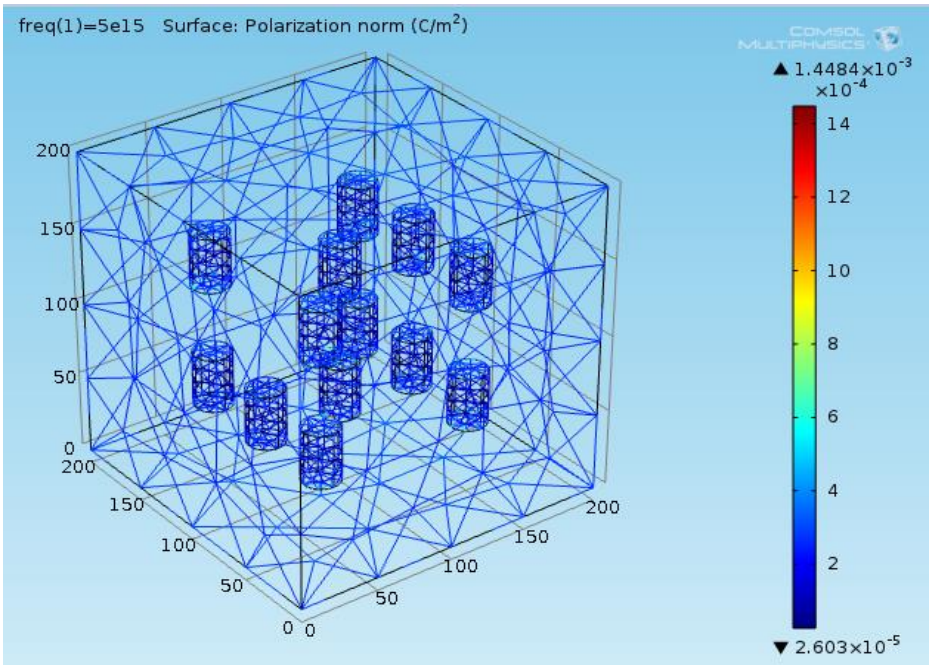

Figure 5.2 c) Surface polarization for cylindrical nanoparticles for f = 0.0225.

The simulation showed that for nanoparticles of constant volume, at a fixed concentration, the surface polarization was highest for spherical particles, and lowest for cylindrical particles. The maximum polarization observed for spheres is $2.019*10^{-3}$ C/m^2, while for ellipsoids it is $1.5558*10^{-3}$ C/m^2, and $1.4484*10^{-3}$ C/m^2 in the case of cylinders. These results validate that spherical nanoparticles generate high surface polarization, and thus high K values among all the other nanoparticles. This is because the spheres have high surface area exposed to the applied electric field compared to other particles. In addition to the surface area, the distribution of nanoparticles in the polymer matrix and the interaction among the particles also plays a major role in the generated polarization. In this simulation, the nanoparticles are assumed to be uniformly distributed; the length of the cylinders is assumed to be along the direction of the applied electric field, and ellipsoids are assumed to be prolate spheroids, in which the polar axis is along the direction of the electric field (without loss of generality). These assumption are made

because the nanoparticles dispersed in polymer matrix can gain any random distribution and the assumed distribution is one of them. The dimensions of the nanoparticles are kept lower than the mean free path of electron in silver (40 nm) in accordance with the Drude-Lorentz model for size dependent nanoparticles.

5.2.2 Effect of the fraction of loading of nanoparticles on surface polarization

To see the effect of loading of nanoparticles in the polymer, models are created for nanodielectric capacitors with varying volume fractions. The same boundary and subdomain conditions as described in Section 3.4 are applied here. Models are created for spherical nanoparticles of diameter 34 nm, at loading fractions of 0.02, 0.03, 0.04, 0.08, 0.12 and 0.154 with n = 8, 12, 16, 32, 47 and 60 nanoparticles respectively. Surface polarization plots are generated for each case and the results are analyzed. The models with respective polarization plots are shown in Figures 5.3 a)-f).

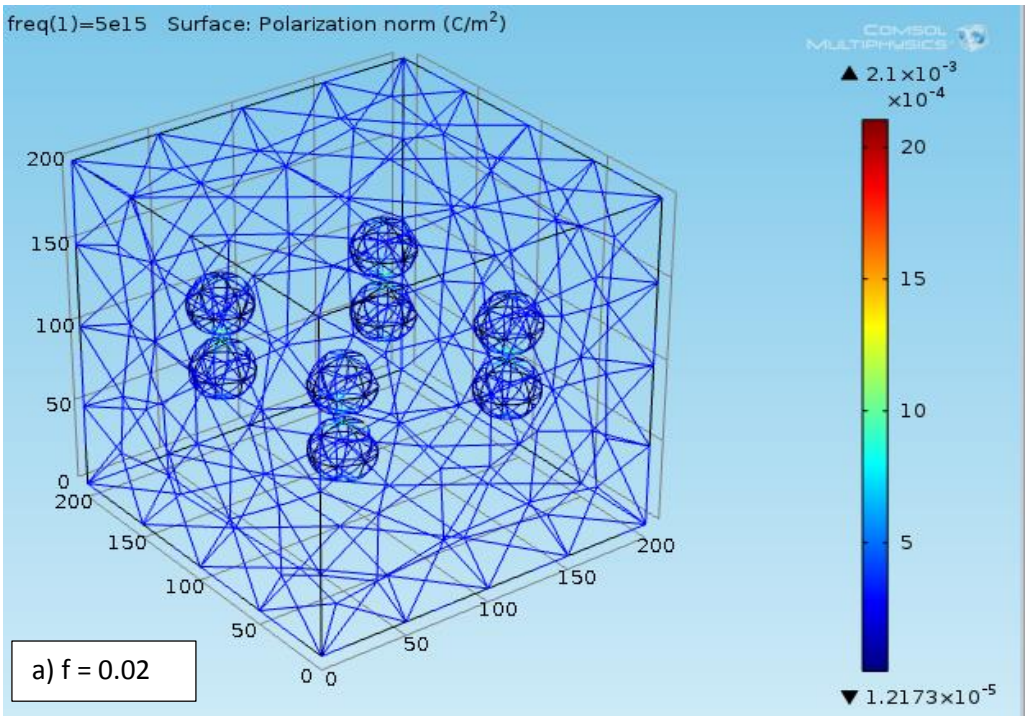

Figure 5.3 Polarization plots for various loadings of nanoparticles, a) f = 0.02.

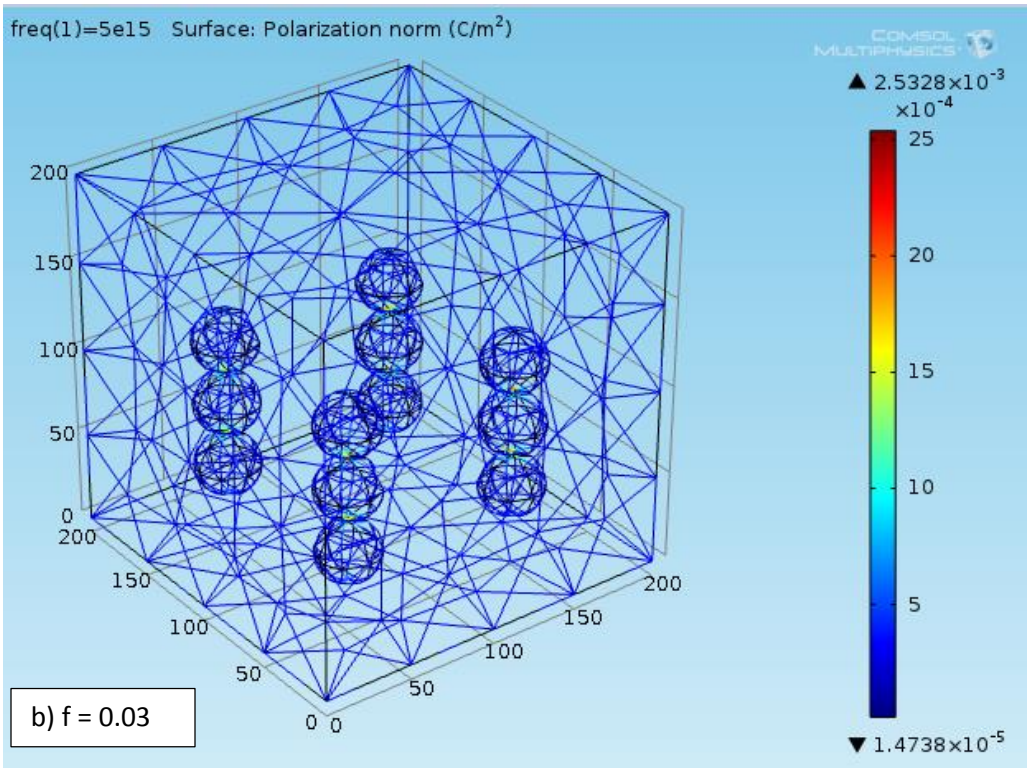

Figure 5.3 Polarization plots for various loadings of nanoparticles, b) f = 0.03.

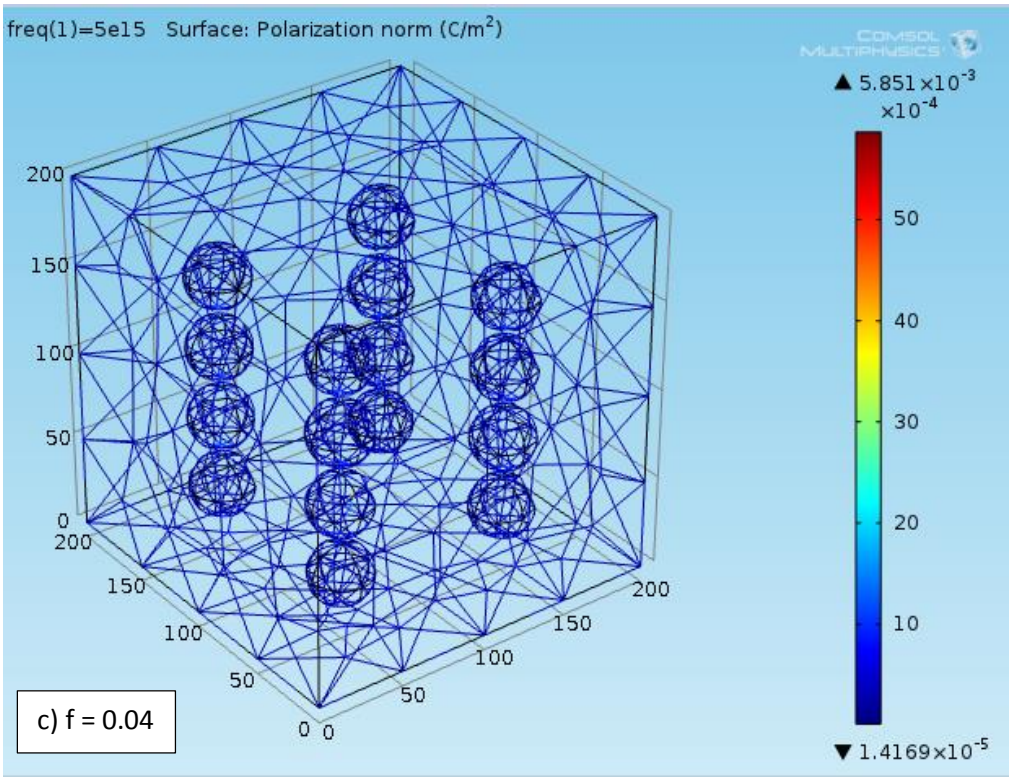

Figure 5.3 Polarization plots for various loadings of nanoparticles, c) f = 0.04.

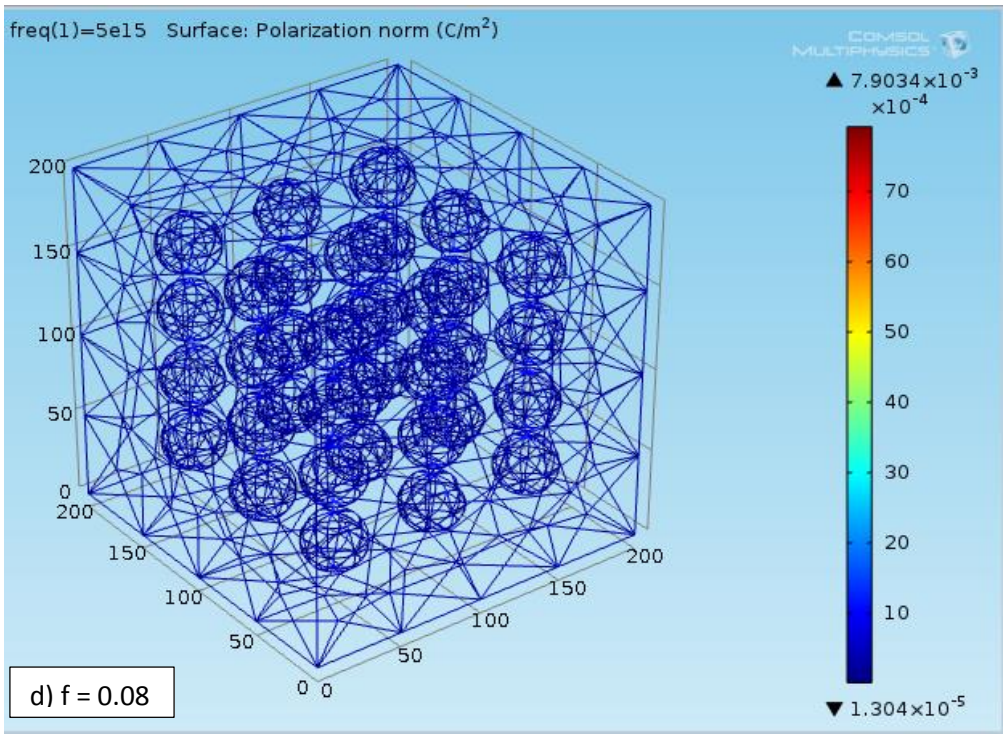

Figure 5.3 Polarization plots for various loadings of nanoparticles, d) f = 0.08.

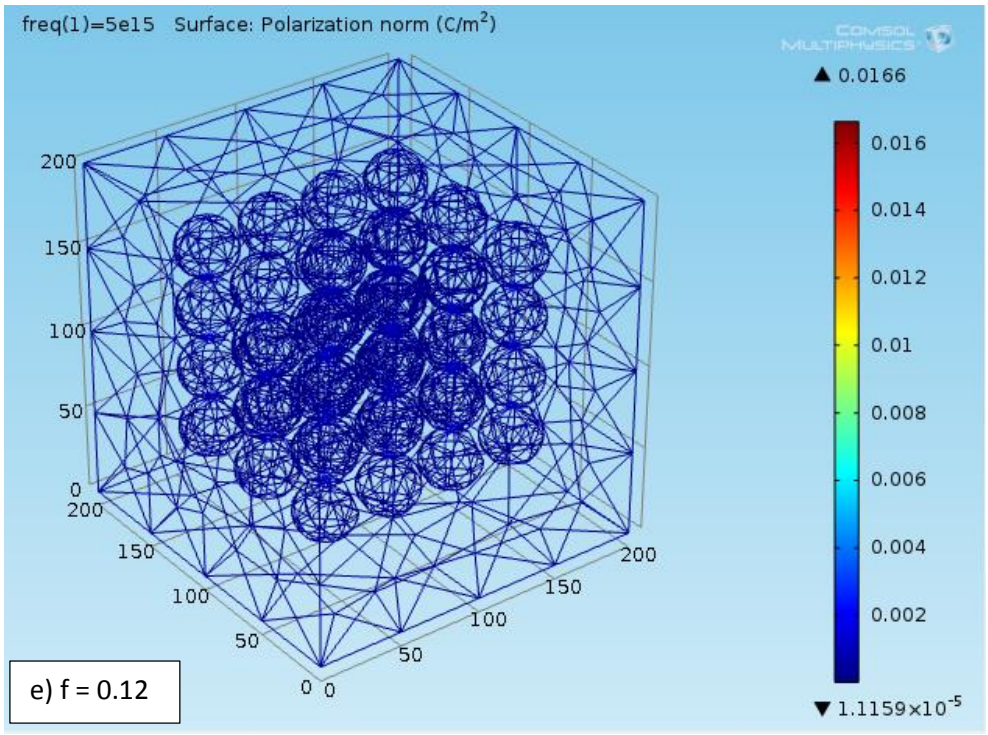

Figure 5.3 Polarization plots for various loadings of nanoparticles, e) f = 0.12.

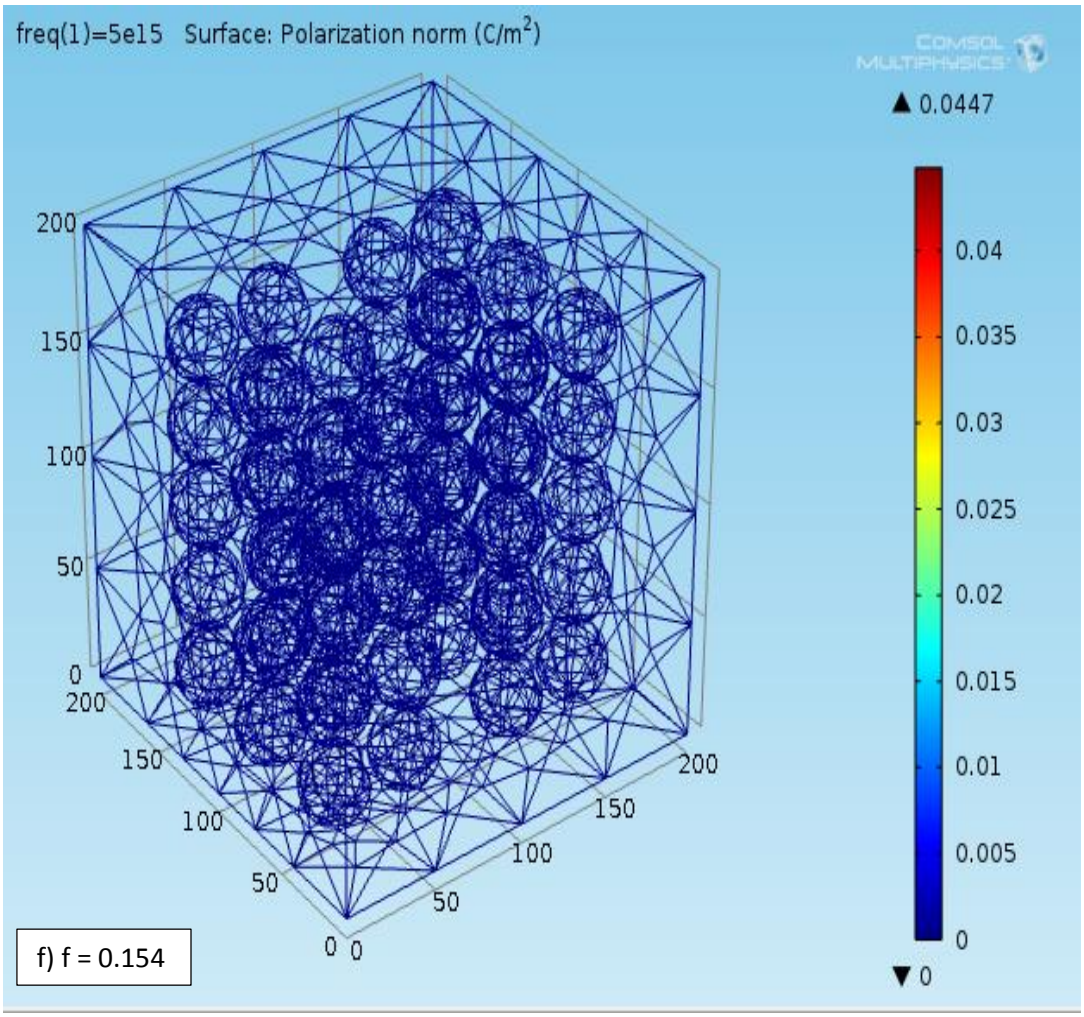

Figure 5.3 Polarization plots for various loadings of nanoparticles, f) f = 0.154.

The graph in Figure 5.4 shows the increase in surface polarization as the concentration of nanoparticles increases, and the polarization reaches the highest near percolation threshold. The increasing trend in polarization is observed because as the number of nanoparticles increase, the surface area available for polarization increases. Since polarization is mainly a surface phenomenon in conductors (metal nanoparticles in this case), this phenomenon is observed.

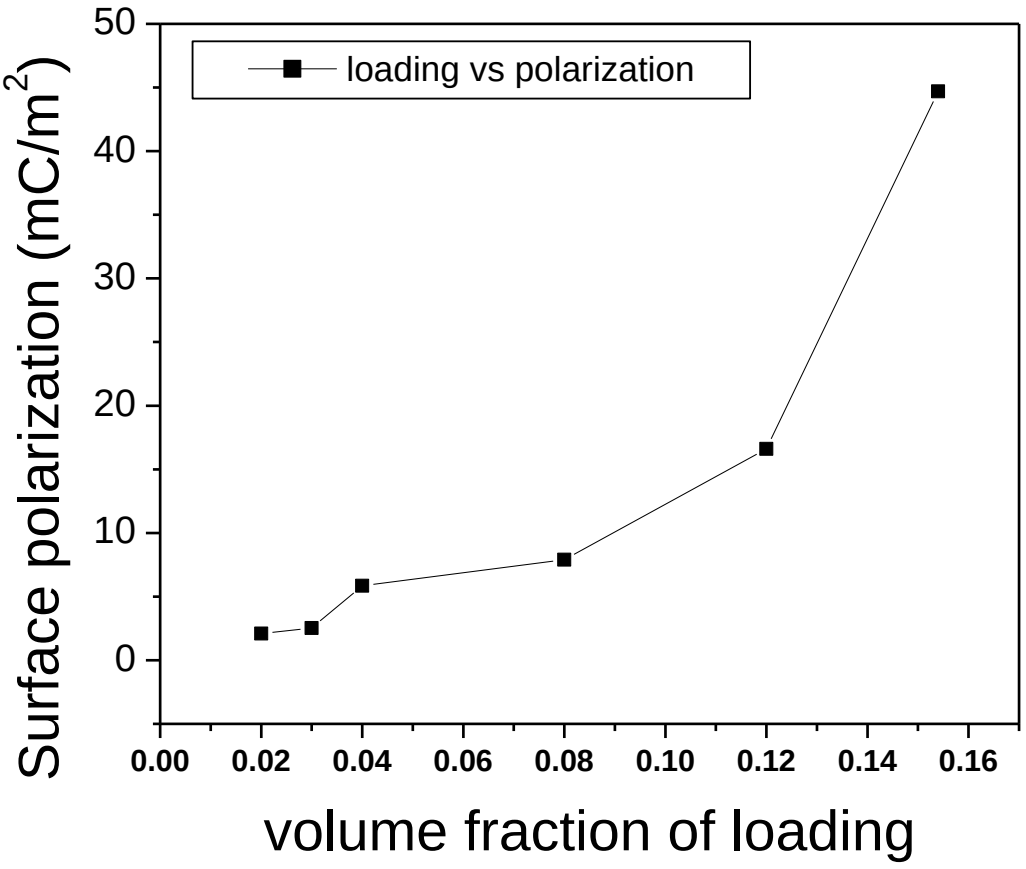

Figure 5.4 Surface polarization plot for various concentrations.

5.2.3 Effect of the size of the nanoparticles on surface polarization

Nanostructures and devices utilize the characteristic effects and phenomena between atoms and clusters of atoms and molecules, mainly surface effects [46]. The ratio of surface area to volume of a sphere is $\frac{3}{r}$, and as the radius of the sphere is reduced, the ratio becomes more and more pronounced. Thus the smaller the spherical nanoparticles the higher the surface area for a given loading of nanoparticles. The effect of size of nanoparticles on the interfacial area is shown in Figure 5.5.

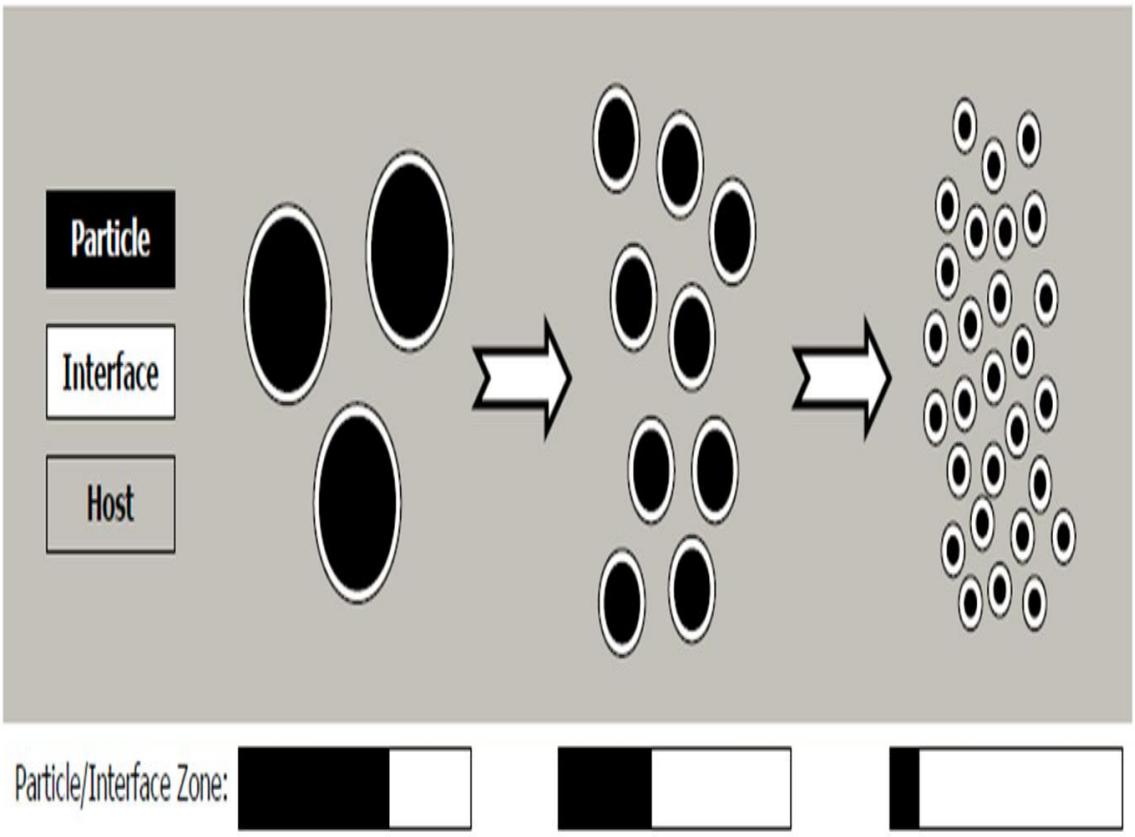

Figure 5.5 Illustration of how the ratio of the filler material to the interfacial area changes with the size of the filler.

To observe the effect of size of nanoparticles on surface polarization, models of nanodielectric capacitors are simulated using particles of various sizes in a polymer block of fixed volume. At a particular fraction of loading (in this case f =0.0225), the diameter of nanoparticles is varied and particles of diameters 35 nm, 30 nm, 24 nm and 20 nm are considered. At a loading of 0.0225, the number of nanoparticles in the block are 8, 13, 22 and 43 respectively. The models and the surface polarization plots in each case are shown in Figures 5.6 a) - d).

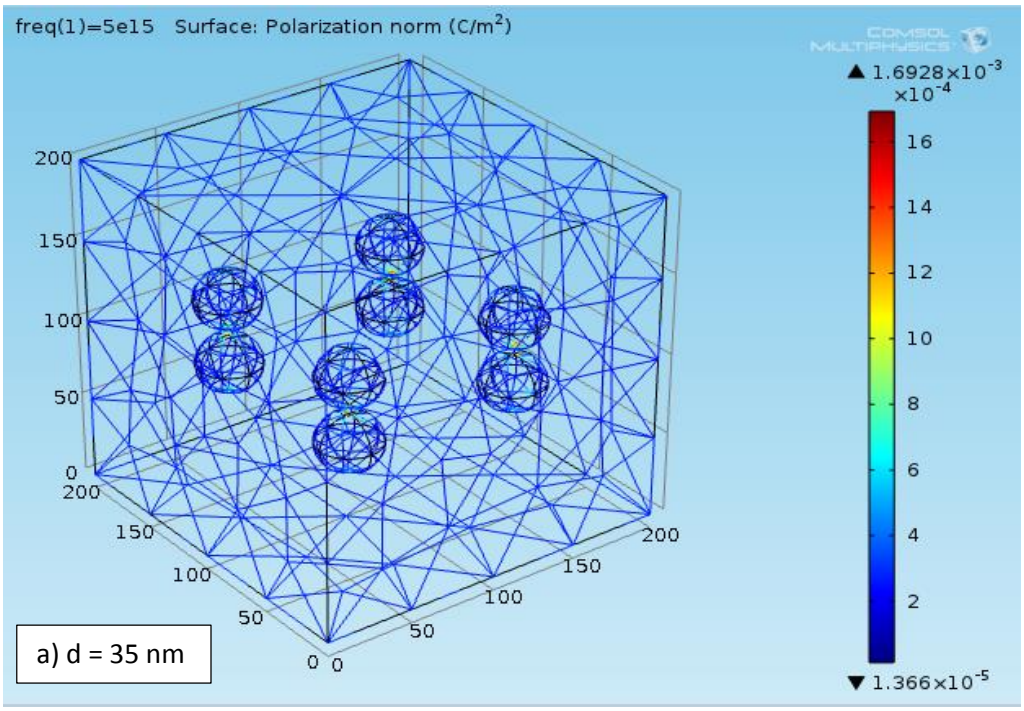

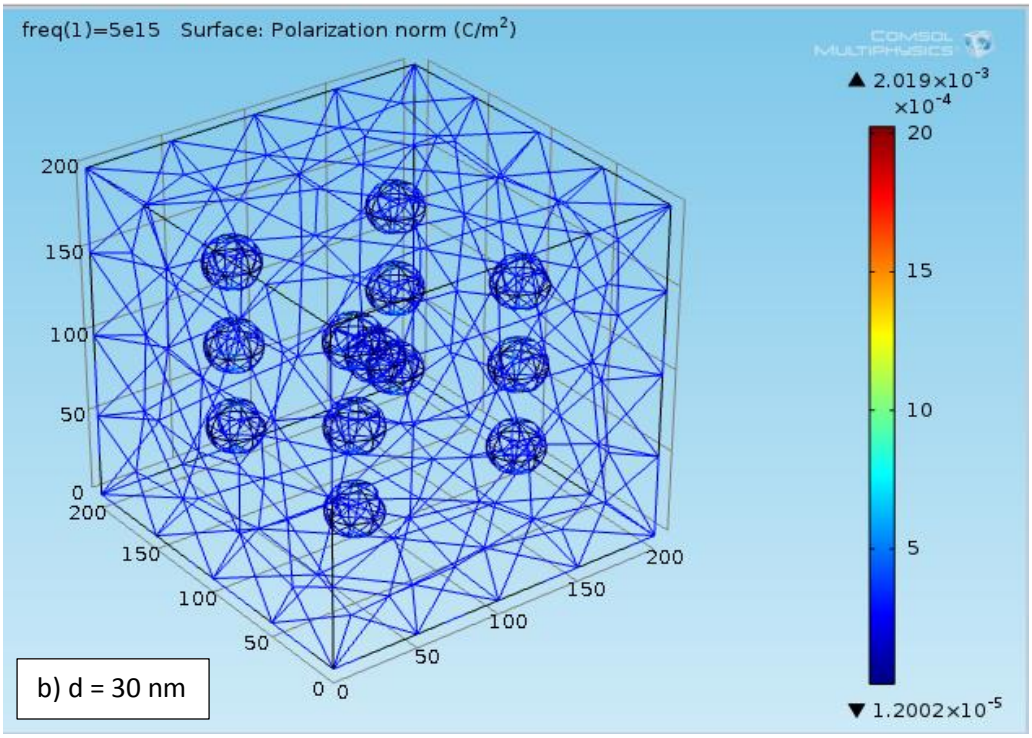

Figure 5.6 Polarization plots for nanoparticles of various sizes at constant fraction of loading, a) d = 35 nm, b) d = 30 nm.

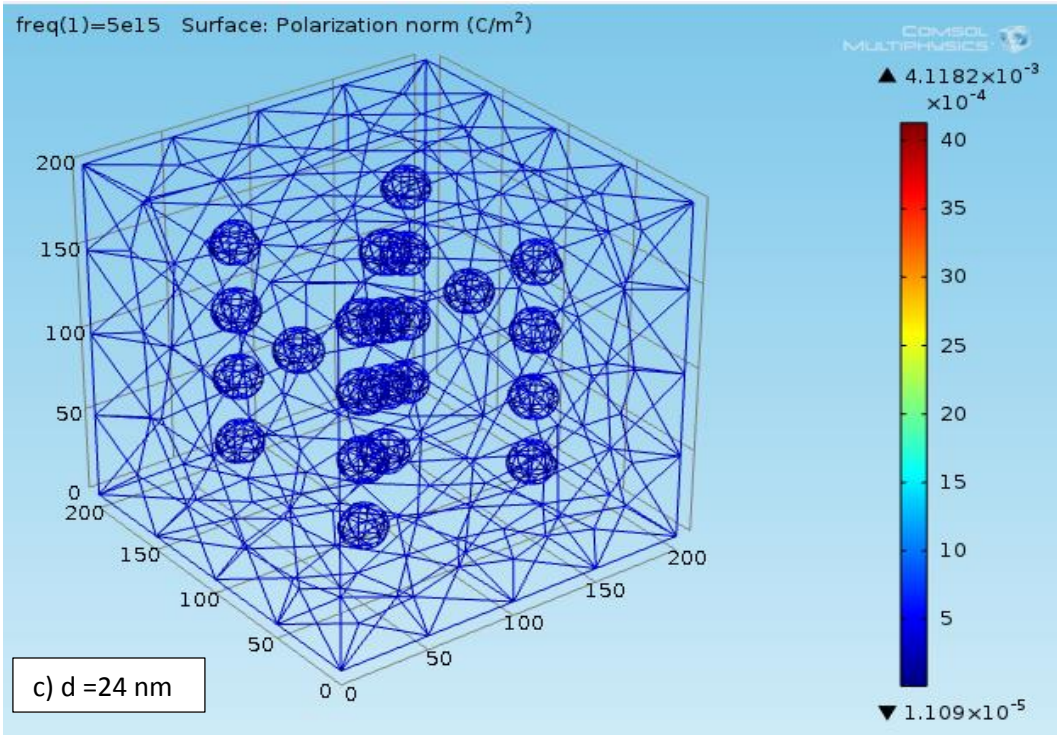

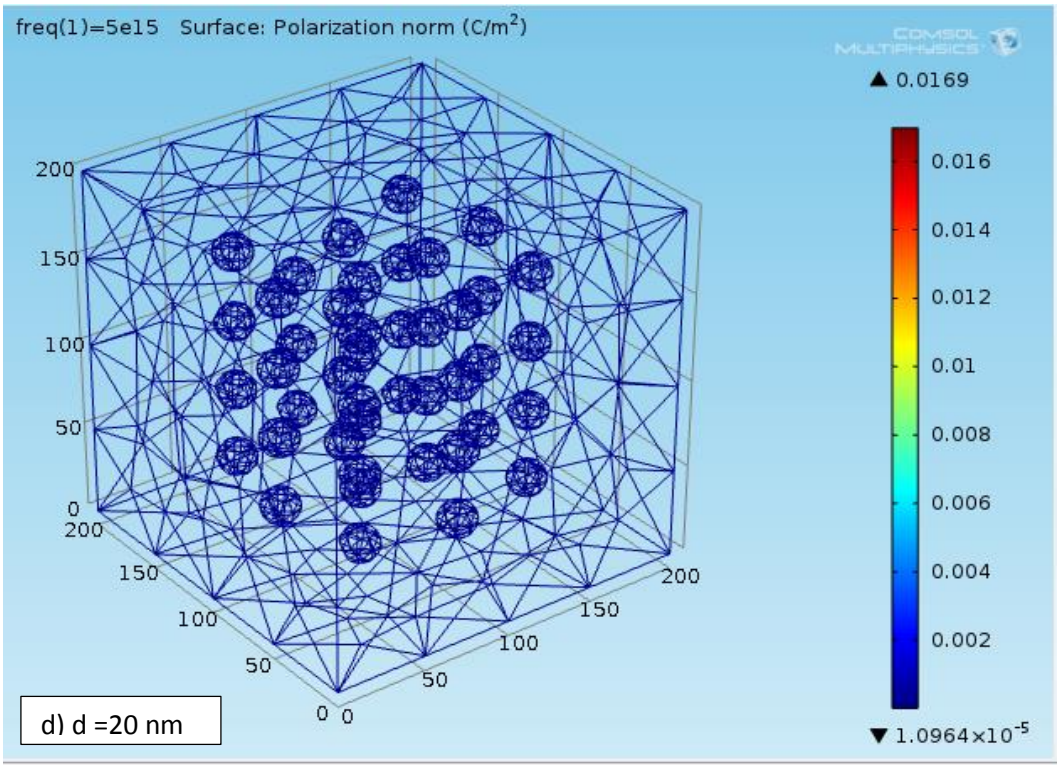

Figure 5.6 Polarization plots for nanoparticles of various sizes at constant fraction of loading, c) d = 24 nm, d) d = 20 nm.

The surface polarization value is found to be increasing with reduction in size and reached 0.0169 C/m^2 for particles of diameter 20 nm, and is lesser in the case of particles of diameter 35 nm with a value of 1.6928*10^{-3} C/m^2. The plot of these values is shown in Figure 5.7.

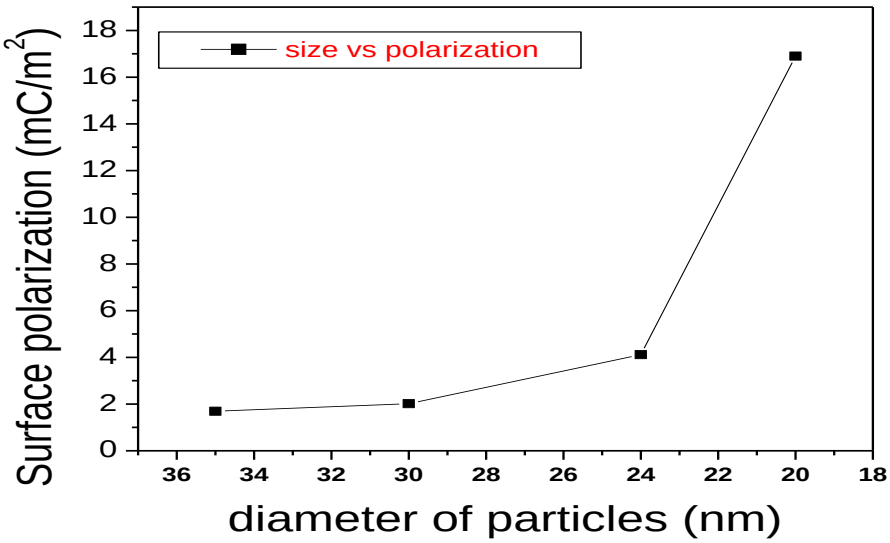

Figure 5.7 Surface polarization plot as a function of size of nanoparticles, at constant loading of f = 0.0225.

The smaller nanoparticles provide large surface area for the applied electric field and result in high surface polarization values. It is important to note here that electric polarization is due to the movement of electrons across the surface in the case of conductors and through the distortion of electron clouds in the case of insulators.

5.3 Experimental results

5.3.1 Effect of the concentration/loading of the nanoparticles on the dielectric properties of the composite

Percolation theory predicts that rapid improvement in k value is observed when the loading reaches a value called the percolation threshold. Sometimes, the effective k of the metal-insulator composite can be three or four times the magnitude of the k of the

insulating matrix. For loadings of Ag nanoparticles in insulating PVP matrix dispersed in ethanol solvent, the percolation threshold is observed at 4% wt. The dielectric constant is found to be nearly 20, for a loading of 4% wt. (refer Figure 4.5). This is around three times the magnitude of the dielectric constant value 7 of PVP. Beyond this loading, the dielectric constant is found to be decreasing because of the formation of conducting paths due to clusters and agglomerations of nanoparticles. Thus, this conductor-insulator composite exhibits percolative behavior as predicted by percolation theory.

5.3.2 Effect of distribution of nanoparticles on the dielectric properties of the composite

The uniform dispersion of nanoparticles in the nanocomposite plays an important role in determining the dielectric properties of the composite. When the nanoparticles form clusters and are agglomerated, they form a conducting path in the composite and no longer act as capacitor. In this work, centrifuge is used to separate the agglomerated nanoparticles by the process of precipitation. The nanocomposite solution is subjected to various centrifugation durations and capacitors are fabricated from each solution. For a centrifugation time of 40 minutes, the samples showed 12.6% increase in capacitance, whereas the samples of 20 minute centrifugation time reported little or no improvement in capacitance. Centrifugation duration beyond this showed no improvement in capacitance.

5.3.3 Control of dielectric properties of high k-composite by employing two different layers of dielectric

By employing two layers of dielectric, we tried to improve the dielectric properties of the overall composite. Using 4% wt. Ag/PVP solution in ethanol as first

layer, and 0.08% wt. Ag/PVP solution in ethanol as second layer, we found that the resulting dielectric showed better properties compared to single layer of 4% wt. Ag/PVP dielectric in ethanol solution. These capacitors showed very stable capacitance performance over 100 Hz-100 kHz range with reduction of only 3% in the entire range. Also, the dissipation factors exhibited by these capacitors are very low (in the range of 0.008-0.001), which means that the capacitors are not lossy.

5.3.4 Charge storage and dielectric properties of the nanodielectric films by realizing parallel connection of capacitors

Parallel connection of capacitors results in higher charger storage and can be used in pulsed power applications. In this work, a design for parallel connection of capacitors using nanodielectric films was conceived and realized. The design was achieved using layers of dielectrics and metal contacts with electrical contact between alternate metal depositions. The fabricated capacitor showed two fold increase in capacitance achieving higher charge storage.

CHAPTER 6. CONCLUSIONS AND FUTURE WORK

6.1 Conclusions

Material design, development and processing of high dielectric constant nanocomposites for embedded capacitor applications are challenging for realization of the embedded passive technology. This work focuses on the study of the design, development and property evaluation of conductive filler/polymer nanocomposites as candidate material for this application. The candidate metal nanoparticles which meet the design needs and the insulating polymer with higher dielectric constant, better dielectric strength and low dissipation factor are selected for this work. Ag nanoparticles have good electrical conductivity and PVP polymer has good dielectric properties compared to other polymers and can dissolve in many polar solvents. The nanocomposite solution is synthesized with Ag nanoparticles in PVP matrix dispersed in ethanol solvent and the dielectric performance is studied for various concentrations, and methods such as layers of dielectric and centrifugal tests were employed. The dielectric behavior of the nanocomposites was studied systematically over a range of frequencies to determine the dependence of dielectric constant, dielectric loss tangent and dielectric strength for different scenarios.

Nanocomposite solutions of various concentrations are prepared and the dielectric properties like capacitance, dissipation factor and dielectric strength were measured. The percolation threshold of the metal-insulator dielectric is observed at 4% loading of Ag nanoparticles in PVP polymer. The dielectric constant is found to be increasing with concentration, and reached a highest value of 19.17 at 4% loading. Beyond this loading, the k value is found to be decreasing following a percolative behavior. Centrifugation test

on 20% wt. nanocomposite showed slight improvement in capacitance. For 40 minutes of centrifugation time, the nanodielectric showed 12.6% improvement in capacitance. A two layer dielectric model using nanocomposites from two different solvents was realized in this work. A 4% wt. Ag/PVP NC in ethanol, and 0.08% wt. Ag/PVP NC in water were used. This two layer dielectric model showed better capacitance over a large frequency range (100 Hz-100 kHz), and also had low dielectric loss. A parallel connection of capacitors using dielectric films and metal depositions is designed in this work to investigate charge storage. A parallel connection of two nanodielectric capacitors was achieved and the sample showed two fold increase in capacitance.

Table 6.1 shows the comparison of dielectric properties of some of the commercially available embedded capacitors with that of the capacitors obtained from this work. The capacitors from this work had thinner dielectric films, exhibited high dielectric constant, and had good dielectric strength and a high capacitance density compared to the commercial embedded capacitors.

Table 6.1 Comparison with commercial embedded capacitors.

Manufacturer	**3M**	**Dupont**	**Oak-Mitsui**	**This work**
Trade name	ECM C2006	Interra HK 04J12	Faradflex MC8TM	Ag/PVP NC
Dielectric material	Ceramic filled epoxy	Polyimide film	Polymer with high k ceramic fillers	Nanoparticle embedded polymer
Thickness	6 µm	12 µm	8 µm	<3 µm
Dielectric constant	22@ 1 kHz	3.5@ 1 MHz	10.5@ 1 MHz	19.99@ 10 kHz
DF	0.010@ 1 kHz	0.005@ 1 MHz	0.020@ 1 MHz	<0.035
Dielectric strength	118.11 V/µm	314.96 V/µm	160 V/µm	>166.67 V/µm
Capacitance density	3.1 nF/cm^2@ 1 kHz	0.26 nF/cm^2@ 1 MHz	1.03 nF/cm^2@ 1 MHz	6.06 nF/cm^2@ 100 kHz

6.2 Future work

High k dielectric materials are always in demand and are receiving great interest in recent years due to their potential applications in gate-dielectrics and high charge storage capacitors [51]. The implementation of high-k gate dielectrics is one of several strategies developed to allow further miniaturization of microelectronic components in semiconductor industry.

Polymer materials with high dielectric constant can be used as the host matrix. High k of the host matrix contributes to the effective k of the composite according to percolation theory. Polyvinylidene fluoride (PVDF), a polymer with k value of 12 can be used as host matrix. Its melting point is 177 ^{0}C and has high dissipation factor around 1.8, and does not dissolve in water. These factors are to be considered while synthesizing nanocomposite solutions. It has been found that addition of surfactant or dispersant such as phosphate esters can improve the dispersion of nanoparticles in polymer matrix and thereby the overall film quality and dielectric performance of the nanocomposites [52]. Those methods can be implemented.

The dispersion of nanoparticles in the nanocomposite and their distribution in the nanodielectric greatly determine the properties of nanodielectric capacitor. Spin coating of nanocomposite solution also contributes to non-uniform distribution of nanoparticles. So instead, inkjet printing methods which print layers of solution on the substrate can be used for forming dielectric. Inkjet printing is found to offer many advantages compared to spin coating such as positional accuracy, large area printing, non-contact method and also low material consumption. It can also print user defined patterns and can print on a range of substrates like rough, smooth and 3D surfaces.

REFERENCES

1. Y. Rao, J. Yue, and C. P Wong, "High K Polymer-Ceramic Nano-Composite Development, Characterization, and Modeling for Embedded Capacitor RF Application," in Proc. of IEEE 51st Electronic Component Technology Conference, pp. 1408–1412, May-June 2001.
2. J. Xu and C. P. Wong, "Effects of the Low Loss Polymers on the Dielectric Behavior of Novel Aluminum-filled High-K Nanocomposites," IEEE 54th Electronic Component and Technology Conference, pp. 496-506, 2004.
3. Richard K. Ulrich, Advanced Electronic Packaging, 2nd Edition, John Wiley & Sons, 2006.
4. R. R. Tummala, E. J. Rymaszewski, and A.G. Klopfenstein, Microelectronics Packaging Handbook, 2nd Edition, Massachusetts: Kluwer Academic Publishers, 1999.
5. R. K. Ulrich and L. W. Schaper, Integrated Passive Component Technology, Hoboken, NJ: IEEE Press, Wiley-Interscience, 2003.
6. "iNEMI (International Electronic Manufacturing Initiatives) 2007 Research Priorities" at http://thor.inemi.org/webdownload/RI/iNEMI_2007_Research_Priorities.pdf.
7. J. Lu, "High Dielectric Constant Polymer Nanocomposites for Embedded Capacitor Applications," School of Material Science and Engineering, Georgia Institute of Technology, Georgia, 2008.
8. J. P. Shaffer, A. Saxena, S. D. Antolovich, T. H. J. Sanders, and S. B. Warner, The Science and Design of Engineering Materials, Boston: McGraw-Hill, 1999.

9. Y. Bai, Z. Y. Cheng, V. Bharti, H. S. Xu and Q. M. Zhang, "High Dielectric-Constant Ceramic-Powder Polymer Composites," *Appl. Phys. Lett.*, Vol. 76, pp. 3804-3806, 2000.
10. Q. M. Zhang, V. Bharti and X. Zhao, "Giant Electrostriction and Relaxor Ferroelectric Behavior in Electron-Irradiated Poly(Vinylidene Fluoride-Trifluofoethylene) Copolymer," *Science*, Vol. 280, pp.2101-2104, 1998.
11. Y. Rao and C. P. Wong, "Material Characterization of a High-Dielectric Constant Polymer-Ceramic Composite for Embedded Capacitor for RF Applications," *J. Appl. Polym. Sci*., Vol. 92, pp. 2228-2231, 2004.
12. Q. M. Zhang, H. F. Li, M. Poh, F. Xia, Z. Y. Cheng and H. S. Xu, "An All-Organic Composite Actuator Material with a High Dielectric Constant," *Nature*, Vol. 419, pp. 284-287, 2002.
13. J. Wang, Q. Shen, C. Yang and Q. Zhang, "High Dielectric Constant Composite of P(VDF-TrFE) with Grafted Copper Phthalocyanine Oligmer," *Macromolecules*, Vol. 37, pp. 2294-2298, 2004.
14. C. Huang, Q. M. Zhang and J. Su, "High Dielectric Constant all Polymer Percolative Composites," *Appl. Phys. Lett*., Vol. 82, pp. 3502-3504, 2003.
15. J. Lu, K. S. Moon, B. K. Kim and C. P. Wong, "High Dielectric Constant Polyaniline/Epoxy Composites via In-situ Polymerization for Embedded Capacitor Applications," *Polymer*, Vol. 48, pp. 1510-1516, 2007.
16. C. Pecharroman, and J. S. Moya, "Experimental Evidence of a Giant Capacitance in Insulator-Conductor Composites at the Percolation Threshold," *Advanced Materials*, Vol. 12, pp. 294-297, 2000.

17. A. E. Neeves and M. N. Birnboim, "Composite Structure for the Enhancement of Nonlinear-Optical Susceptibility," *J.Opt Soc. Am. B*, Vol. 6, No. 4, pp. 787-796, April 1989.
18. K. C. See, J. B. Spicer, J. Brupbacher, D. Zhang and T.G. Vargo, "Modeling Interband Transitions in Silver Nanoparticle-Fluoropolymer Composites," *J. Phys. Chem. B*, Vol. 109, No. 7, pp. 2693-2698, 2005.
19. E. A Coronado and G. C Schatz, "Surface Plasmon Broadening for Arbitrary Shape Nanoparticles: A Geometry Probability Approach," *J. Chem. Pys*, Vol. 119, No. 7, 2003.
20. C. F. Bohren and D. R. Huffman, Absorption and Scattering of Light by Small Particles (Wiley, New York, 1983), p. 258.
21. M. Scheller, C. Jansen and M. Koch, "Applications of Effective Medium Theories in the Tetra Hertz Regime," *Recent Optical and Photonic Technologies*, 2010.
22. W. M. Merrill, R. E. Diaz, M. C. Squires and N. G. Alexopoulos, "Effective Medium Theories for Artificial Materials Composed of Multiple Sizes of Spherical Inclusions in a Host Continuum," IEEE Transactions on Antennas and Propagation, Vol. 47, No. 1, pp. 142-148, 1999.
23. C. Pecharroman and J. S. Moya, "Experimental Evidence of a Giant Capacitance in Insulator-Conductor Composites at the Percolation Threshold," *Advanced Materials*, 12 (4), 294-297 (2000).
24. J. Xu and C.P Wong, " Effects of the Low Loss Polymers on the Dielectric Behavior of Novel Aluminum filled High K Nano-composites," Electronic Components and Technology Conference, Vol. 1, pp. 496-506, 2004.

25. D. S. McLachlan, I.I. Oblakova, and A.B. Pakhomov, "The Complex Dielectric Constant of a Metal (Superconductor)-Insulator System near the Percolation Threshold," *Physica B*, 194-196, 2001-2002 (1994).
26. D. W. Pepper and J. C. Heinrich, The Finite Element Method: Basic Concepts and Applications, Hemisphere Publishing Corporation, USA, 1992.
27. G. R. Liu and S. S. Quek, The Finite Element Method: A Practical Course, Elsevier Butterworth-Heinemann, Burlington, 2003.
28. N. W. Ashcroft, and N. D Mermin, Solid State Physics, Saunders College Publishing, 1st edition, 1976.
29. P. B. Johnson and R. W. Christy, "Optical Constants of the Noble Metals," *Phys. Rev. B*, pp. 4370-4379, 1972.
30. U. Kreibig and C.V. Fragstein, "The Limitation of Electron Mean Free Path in Small Silver Particles," *Zeitschrift für Physik*, Vol. 224, Issue 4, pp. 307-323, 1969.
31. X. Zhang, Y. L. Chen, R. Liu and D. P Tsa, "Plasmonic Photocatalysis," *Rep. Prog. Phys*. Vol.76, pp. 046401-1–046401-41, 2013.
32. L. Nicolais and G. Carotenuto, Metal-Polymer Nanocomposites. John Wiley & Sons Inc.: Hoboken, NJ, 2005.
33. M. Rabuffi and G. Picci, "Status Quo and Future Prospects for Metallized Polypropylene Energy Storage Capacitors," IEEE Transactions on Plasma Science, Vol. 30, pp. 1939-1942, 2002.
34. Y. Sun and Y. Xia, "Shape Controlled Synthesis of Gold and Silver Nanoparticles," *Science*, Vol. 298, Issue 5601, pp. 2176-2179, 2002.
35. C. J Murphy, *Science*, 298, 2139, 2002.

36. C. W. Nan, Y. Shen and J. Ma, “Physical Properties of Composites near Percolation,” *Annu. Rev. Mater*. Res, 40, 3.1–3.21, 2010.
37. R. J. Romano, “Contact Angles,” University of Massachusetts, Lowell, 2006.
38. J. Drelich, J. L. Wlibur, J. D. Miller and G. M. Whitesides, “Contact Angles for Liquid Drops at a Model Heterogeneous Surface Consisting of Alternating and Parallel Hydrophobic/Hydrophilic Strips,” *Langmuir*, Vol. 12, pp. 1913-1922, 1996.
39. K. Hermansson, U. Lindberg, B. Hok, and G. Palmskog, “Wetting Properties of Silicon Wafers,” *Transducers '91*, pp. 193-196, 1991.
40. S. J. Spencer, G. T. Andrews and C. G. Deacon, “Contact Angle of Ethanol–Water Solutions on Crystalline and Mesoporous Silicon,” *Semicond. Sci. Technol*. Vol. 28 (pp. 5), 2013.
41. M. Reading and A. S. Vaughan, “Dispersion and Rheology of Poly(ethylene oxide)/MMT Nanocomposites,” IEEE Conf. Electr. Insul. Dielectr. Phenomena (CEIDP), pp. 37-40, 2008.
42. L. Hui, R. C. Smith, X. Wang, J. K. Nelson and L. S. Schadler, “Quantification of Particulate Mixing in Nanocomposites,” IEEE Conf. Electr. Insul. Dielectr. Phenomena (CEIDP), pp. 317-320, 2008.
43. M. Kurimoto, H. Watanabe, K. Kato, M. Hanai, Y. Hoshina, M. Takei and H. Okubo, “Dielectric Properties of Epoxy/Alumina Nanocomposite Influenced by Particle Dispersibility,” IEEE Conf. Electr. Insul. Dielectr. Phenomena (CEIDP), pp. 706-709, 2008.
44. C. Green and A. Vaughan, “Nanodielectrics – How Much Do We Really Understand?,” IEEE Electr. Insul. Mag., Vol. 24, No. 4, pp. 6-16, 2008.

45. M. E. Deepak, “Design and Fabrication of Metal-Polymer based Core-Shell Artificial Nanodielectrics for Embedded Capacitor Applications,” University of Houston, Masters Thesis, 2012.
46. Thomas Andritsch, “Epoxy Based Nanodielectrics for High Voltage DC-Applications –Synthesis, Dielectric Properties and Space Charge Dynamics,” Doctoral Thesis, Nov 2010.
47. A. L. Efros and B. I. Shklovskii, *Phys. Status Solidi* (B), 76, 475 (1976).
48. S. Kirkpatrick. *Rev. Mod. Phys*., 45, 574, (1973).
49. D. Staffer, *Phys. Rep*., 54, 3, (1979).
50. D. Wilkinson and J. S. Langer, *Phys. Rev. B: Condense. Matter*, 28, 1081, (1983).
51. J. Lu and C. P Wong, “Recent Advances in High-k Nanocomposite Materials for Embedded Capacitor Applications,” IEEE Transactions on Dielectrics and Electrical Insulation, Vol. 15, Issue 5, pp. 1322-1328, 2008.
52. S. K. Bhattacharya and R. R. Tummala, “Next Generation Integral Passives: Materials, Processes, and Integration of Resistors and Capacitors on PWB Substrates,” *Journal of Materials Science: Materials in Electronics*, Vol. 11, pp. 253-268, 2000.